Dear reviewer

Thank you very much for providing comments. Your suggestions are helpful for improving the manuscript. In the following, we address all comments point-by-point.

> ***Comment 1:*** *The title could be edited more suitably for the main purpose of the paper. In the title, "hydrological modeling and GCMs" expressions could be used.*

Answer:

According to the opinions of reviewers, we have modified paper title to "A 439-year simulated daily discharge dataset (1861-2299) for the upper Yangtze River, China".

> ***Comment 2:*** *In the abstract; the objective, the original value and the widespread impact of the study could be expressed better, the introduction could be handled for meaning unity and logical continuity.*

Answer:

Thank for your suggestion, we tried to express better the objective, value and the widespraed impact of the study in the abstract and modified some sentences in the introduction.

1. Abstract:

"The long-term daily discharge dataset could be used in the international context and water management, e.g. in the framework of Inter-Sectoral Impact Model Intercomparison Project (ISIMIP) by providing clue to what extent human-induced climate change could impact streamflow and streamflow trend in the future."

2. We rewrote some sentences in the introduction:

"Global warming is the long-term rise in average temperature of the earth's climate system. Warming temperature alters global water circulation processes and could significantly influence the sustainability of society and economy (Jung et al., 2011). The variation in water resources availability in the context of global warming is acknowledged as a focus of many international research projects (Stagl et al., 2016; Raman et al., 2018; Maisa et al., 2019). The long-term accurate (as much as possible) daily discharge time series are crucial for in-depth understanding of the changes in streamflow, and they are needed for subsequent climate change impact studies. However, discharge is monitored usually only for short observational periods in most river basins.

For generation of the long-term streamflow series, many data mining techniques including the sedimentological method, the hydrological field survey method, and the documentary analysis method can be applied (Longfield et al., 2018). Nevertheless, low temporal resolution and insufficient accuracy of these estimations can hardly meet the demands of practical and research applications. Instead, the observed climatic variables and the outputs of climate models have often been used to drive hydrological models to evaluate changes in streamflow in the context of climate change (Braud et al., 2010; Chen et al., 2017; Su et al., 2017; Dahl, 2018; Seneviratne et al., 2018).

But there is lack of research on the quantitative estimation of long-term streamflow for period longer than 400 years under different scenarios with and without anthropogenic climate change (Meaurio, 2017).

The Yangtze River is the longest river in China. It originates from the Tibetan Plateau and enters the East China Sea after flowing through 11 provinces. With a large topographic gradient and substantial water supply of approximately 10,000 m^3s^{-1} on the average, the upper Yangtze River is rich in hydropower resources, but subjected to destructive flash floods. The Yangtze River has the longest hydrological observations in China. Data provided by the Cuntan hydrological station, which started operating in 1939, facilitates hydro-meteorological studies in the instrumental period (Su et al., 2008; Wang et al., 2008; Su et al., 2017). As changes in streamflow at the Cuntan station directly influence inflow to the Three Gorges Reservoir, establishing long-term discharge series at the Cuntan station can support effective management of hydraulic projects. Besides, the longer discharge series can also provide a possibility to explore impacts of anthropogenic climate change on hydrology for international climate change research community. Therefore, we simulated daily discharge at the Cuntan hydrological station in the upper Yangtze River in the period 1861 - 2299 using available climate model outputs.

The outputs of four downscaled GCMs (GFDL-ESM2M, HadGEM2-ES, IPSL-CM5A-LR, and MIROC5) are utilized to drive four hydrological models (HBV, SWAT, SWIM and VIC) to simulate discharge at the Cuntan station. The climate forcing comprise (a) the scenario with anthropogenic climate change for the period 1861 - 2299, which is subdivided into the historical period (1861 - 2005) and the future period (2006 - 2299) under different Representative Concentration Pathways (RCPs), and (b) the preindustrial control scenario (piControl) for the period 1861 - 2299, which is used as a reference to detect the influence of anthropogenic climate change on streamflow in the upper Yangtze River."

Comment 3: *In the section of study area, Fig. 1 must be pointed out and river basin characteristics (elevation, slope, aspect, land cover, soil type, etc.) must be given shortly to understand the hydrological cycle of the basin.*

Answer:

As suggested by the reviewer, the elevation, slope, aspect meteorological station, land cover and soil type are added to the Fig.1, and explanations are added to section of Study Area in the revised manuscript. The text is as follows:

"The catchment area of the Cuntan hydrological station (29 ° 37 ′ N, 106 ° 36 ′ E) in the upper Yangtze River is approximately 860,000 km^2, and 352.7 billion m^3 water is flowing through this point annually with average discharge of 109,34 m^{3}s^{-1} in the period of instrumental measurements beginning in 1939. Location of the Cuntan hydrological station, 311 GCM grids, meteorological stations and spatial distribution of the land use and soil types in the upper Yangtze River basin are shown in Fig. 1. Prairie grassland and acid purple soil are the most widespread of land use and soil type in the upper Yangtze River basin. The upper Yangtze River has complex geomorphic types and broken topography. Mountains and plateaus can be found in most parts of the region, hills and plains are few. Influenced by the East Asia subtropical monsoon and a complex topography, climate varies across the basin with annual air temperature and precipitation being high in the southeast but low in the northwest headstream region. According to observational data, the areal averaged annual mean temperature and precipitation are 12.3 ℃ and 1018 mm, respectively, in the period 1961 - 2017 in the upper Yangtze River basin."

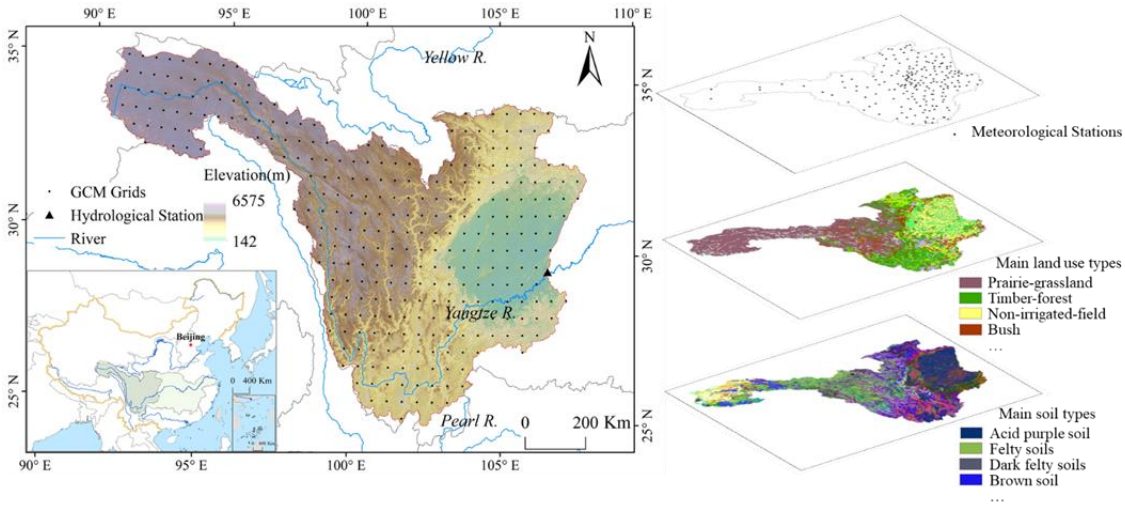

Figure 1 Location of the Cuntan hydrological station, GCM grids, meteorological stations and spatial distribution of the land use and soil types in the upper Yangtze River basin

Comment 4: *In the methods, a flowchart included all processes could be given for the sake of clarity. Moreover, GIS and remote sensing techniques used could be mentioned shortly in this section.*

Answer:

We made a flowchart included all processes for the sake of clarity and added references about hydrological models. See in section 3.4 (page 4-5) as follow:

"Four hydrological models, HBV (Bergstrom et al., 1973), SWAT (Arnold et al., 1998), SWIM (Krysanova et al., 2005) and VIC (Liang et al., 1994) are used to simulate river discharge at the Cuntan hydrological station, and a flowchart of the hydrological modelling process is shown in Fig. 2."

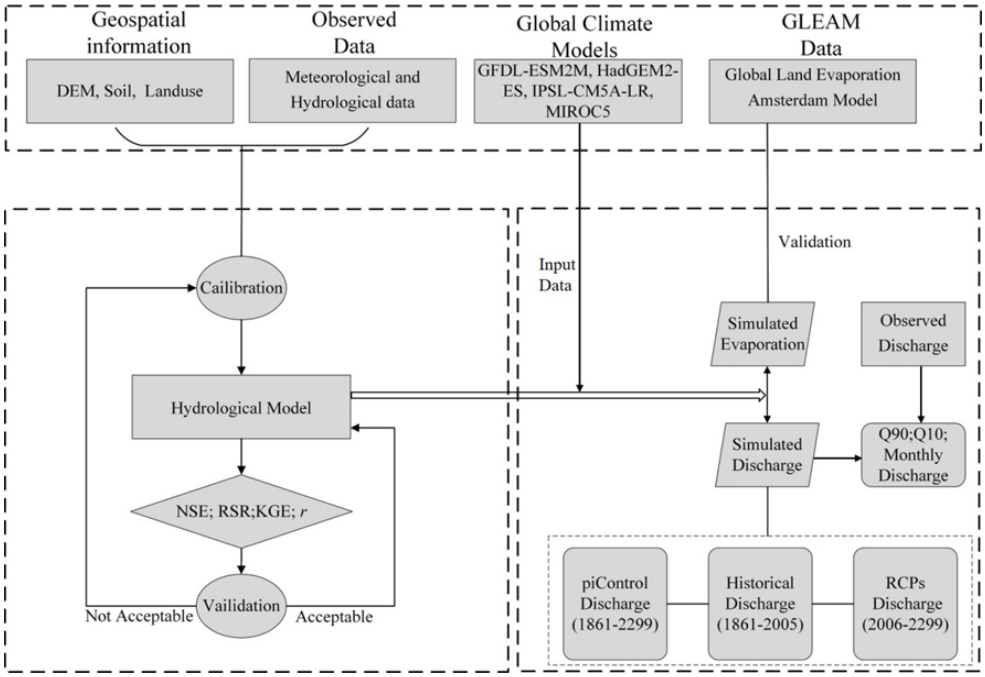

Figure 2 Flowchart of the hydrological modelling process

We made an improper express and caused a misunderstanding about the sentence "The remote sensing data were assimilated to obtain monthly evapotranspiration with a spatial resolution of 0.25°". The remote sensing data is evapotranspiration data, which was produced by mean of remoting sensing techniques. In our study, we compare simulated outputs and GLEAM by means of GIS tools. See discription in section 3.3 as follow:

"Evapotranspiration data from the Global Land Evaporation Amsterdam Model (GLEAM) for 1986 - 2005 that were released by the University of Bristol (Miralles et al., 2011) are used in our study to cross-check the performances of the hydrological models by means of the geographic information system (GIS) tools. The GLEAM data was generated based on a variety of satellite-sensor products at monthly scale with a spatial resolution of 0.25°. The spatial distributions of simulated

evapotranspiration with that from GLEAM are compared by GIS techniques, and kappa value of confusion matrix is also applied to evaluate the accuracy of simulated evapotranspiration (taking VIC output as an example) by refer to GLEAM."

> ***Comment 5:*** *In section 3.1, some information about downscaling, bias correction and data assimilation processes (details, techniques, etc.) of GCMs should be given. And it should be explained that how GCMs grid data was inputted into the hydrological models (as lumped data?). In addition, more details about GCMs (model structures, etc.) and RCP scenarios should be presented.*

Answer:

1. The four GCMs used in this study were widely used in previous studies. The details of them can be obtained from the classical references: Taylor et al. (2012) for GFDL-ESM2M, Jones et al. (2011) for HadGEM2-ES, Dufresne et al. (2013) for IPSL-CM5A-LR and Watanabe et al. (2010) for MIROC5. As a result, we decided not to include a detailed description to keep the paper within a reasonable length.

2. The description of downscaling, bias correction and data assimilation processes can be found in section 3.1 Climate scenarios (page 3, lines 10-19). We also add references for them in case readers would be interested in detail. They are:

Frieler, K., Lange, S., Piontek, F., et al: Assessing the impacts of 1.5 °C global warming – simulation protocol of the Inter-Sectoral Impact Model Intercomparison Project (ISIMIP2b), Geosci. Model Dev., 10, 4321-4345, https://doi.org/10.5194/gmd-10-4321-2017, 2017.

Lange, S.: Bias correction of surface downwelling longwave and shortwave radiation for the EWEMBI dataset, Earth. Syst. Dynam., 9, 627-645, https://doi.org/10.5194/esd-2017-81, 2018.

3. GCMs data are inputted to the hydrological models using data in grid format based on the needs of hydrological models Since the main purpose of this paper is to discuss the discharge dataset and not hydrological modelling, we gave a brief introduction of 4 hydrological models (see Table 2). More details can be found in the Hattermann et al. (2017).

Comment 6: *In section 3.2, please provide details (precipitation, temperature, etc.) of observed daily meteorological data and explain how the data of 189 ground-based stations was inputted into the hydrological models (mean or spatial interpolation/extrapolation of the data?). Furthermore, please give reference/references of flood events (1870 and 1931) because of measurements beginning in 1939.*

Answer:

1. The observed daily meteorological data are derived from the National Meteorological Information Centre of China Meteorological Administration (http://data.cma.cn/). The daily data from 189 ground-based stations are inputted into the hydrological models after interpolation. We added explanations in revised manuscript to make this clear.

"The observed daily meteorological data for 1951 - 2017 from 189 ground-based stations in the upper Yangtze River Basin used in this study were quality controlled by considering changes in instrument type, station relocations, and trace biases at the National Meteorological Information Centre of China Meteorological Administration (Ren et al., 2010), which was inputted into the hydrological models by spatial interpolation. During 1951 - 2017, annual precipitation shows a decreasing trend, with multi-year average of 935 mm, and annual mean temperature has shown a positive trend with multi-year average of 10.5 ℃."

2. Following references are added to cite the flood events (1870 and 1931) (Page 4, lines 5-10):

Changjiang Water Resources Commission of the Ministry of Water Resources: The flood and drought disasters in the Yangtze River Basin, China Water & Power Press, Beijing, China, 2002.

Hu, M.S. and Luo, C.Z: The historical flood of China, China Bookstore press, Beijing, China, 1992.

Luo, C.Z. and Le, J.X: The flood of China, China Bookstore press, Beijing, China, 1996.

Comment 7: *In section 3.3, please give more details about GLEAM and the assimilation technique. And please present the comparison results of GLEAM and 4 hydrological models for internal consistency of the models in the results section.*

Answer:

1. Evapotranspiration data from the Global Land Evaporation Amsterdam Model (GLEAM) for 1986 - 2005 that were released by the University of Bristol (Miralles et al., 2011) is used to cross-check performances of the hydrological models. The GLEAM data was generated based on a variety of satellite-sensor products at monthly scale with a spatial resolution of 0.25°. For more details please refer to Miralles et al., 2011 (Section 3.3, page 4). We also added explanations in revised manuscript to clarify this.

2. Besides, we compare results of GLEAM and 4 hydrological models for checking the internal consistency of the models in the section 4.2 Calibration and validation of the hydrological models (Section 4.2, page 7 and Fig. 8) as follows:

“In addition, evapotranspiration outputs of HBV, SWAT, SWIM, VIC are compared with the GLEAM evapotranspiration data (see Section 3.3) in the period 1986 - 2005. The long-term averaged annual evapotranspiration simulated by the four models for the upper Yangtze River basin is 442 mm, 487 mm, 484 mm, 466 mm, respectively, quite close to the result from GLEAM (452 mm). The spatial patterns of the gridded evapotranspiration outputs of the HBV, SWAT, SWIM, VIC model and GLEAM all show low values in the northwest but high values in the southeast of the upper Yangtze River basin (Fig. 8). Furthermore, a matrix consisting of 500 randomly selected pixels from simulated evapotranspiration by VIC and corresponding GLEAM grids is set up to get the kappa value. The deduced kappa value of 0.62 indicates a substantial agreement of two date sources.”

> ***Comment 8:*** *In section 3.4, please present input and output data of the models, model structures (loss and transform methods, soil moisture accounting, snow melting-accumulation, evapotranspiration, groundwater, canopy interception etc.) and parameter sets.*

Answer:

The input and output data of this study are the Global Climate Models (GFDL-ESM2M, HadGEM2-ES, IPSL-CM5A-LR and MIROC5) and simulated discharge (https://doi.org/10.4121/uuid:8658b22a-8f98-4043-9f8f-d77684d58cbc), respectively.
The hydrological processes including loss and transform methods, soil moisture accounting, snow melting and accumulation, groundwater-related processes, canopy interception etc, can be found in the references related with the HBV (Bergstrom et al., 1973), SWAT (Arnold et al., 1998), SWIM (Krysanova et al., 2005) and VIC (Liang et al., 1994). The references are included.

Comment 9: *In section 3.5, please indicate how many parameters were calibrated for each model and what is the range for each parameter.*

Answer:

Thank you for your suggestion. Ranges of parameters need to be calibrated are included in Table 3 to respond your request.

Table 3 The parameters and their ranges used for calibration of four hydrological models

HBV		SWAT		SWIM		VIC	
Name	Range	Name	Range	Name	Range	Name	Range
Threshold quick runoff (UZ1)	0-100	Deep aquifer percolation fraction (*Rchrg_Dp*)	0-1	Routing coefficient 1 (*roc1*)	1-100	Non-linear baseflow begins (*Ds*)	0-1
Percolation to lower zone (*PREC*)	0-6	Saturated hydraulic conductivity (*Sol_K*)	0-100	Routing coefficient 2 (*roc2*)	1-100	Maximum baseflow (Ds_{max})	0-30
Non-linearity in soil water zone (*BETA*)	1-5	Maximum canopy storage (*Canmx*)	0-10	Evaporation coefficient (*thc*)	0.5-1.5	Maximum soil moisture (*Ws*)	0-1
Slow time constant upper zone (*KUZ1*)	0.01-1	Average slope steepness (*Slope*)	0-0.6	Baseflow factor for return flow travel time (*bff*)	0.2-1	Variable Infiltration Capacity curve (b_i)	0-0.4
Additional precipitation coefficient for snow at gauge (*SKORR*)	1-3	Available water capacity (*Sol_Awc*)	0-1	Coefficient to correct channel width (*chwc0*)	0.1-1	Soil depth 1 (d_1)	0.1-1
Precipitation correction for rain (*PKORR*)	0.8-3	Initial SCS CN II value (*Cn2*)	35-98	Saturated conductivity (*sccor*)	0.01-10	Soil depth 2 (d_2)	0.1-2
		Groundwater "revap" coefficient (*Gw_Revap*)	0.02-0.2	Groundwater recession rate (*abf*)	0.01-1	Soil depth 3 (d_3)	0.1-3
		Biological mixing efficiency (*Biomix*)	0-1	Initial conditions (*gwq0*)	0.01-1		
		Soil evaporation compensation factor (*Esco*)	0-1	Curve number (*cnum*)	10-100		

Comment 10: *In section 3.6, please clarify the problem of "is the use of 1990 year land use convenient for particularly future scenarios?". In conclusions and discussion section, it is stated that 1990-year land use is one of the uncertainties and human interferences have escalated since the 1990s. In my opinion, using 1990 land use data is a big handicap of this study that is not convenient for future modeling. 1990 land use data can be considered suitable for only piControl and historical periods. Modeling of future flows by using the land cover of 1990, when the industrial development has not started, will have misleading results, especially in human impact scenarios. The use of 2019 year land cover data would be more appropriate when modeling the future and this will make the results more consistent. I don't accept the pretext of not available by reason of the fact that current land use data can be easily obtained from various sources*

Answer:

Thank you for your valuable comment and suggestions. We cannot deny that the newest land cover data may be more appropriate for simulating future discharge. However, it still cannot represent the land cover in the future. Therefore, we tried to use data, including land cover, reflecting the whole calibration/validation period, which would reduce uncertainty except for climate change. The calibration period is 1979-1990, thus, we used the 1990 land use as single geographical data to simulate the daily discharge.

In the previous study (Su et al., 2016, as follow) the 1990 land use map was used for simulating the discharge for the upper Yangtze River, China, and other previous studies showed that impact of land use on stream flow is rather small (Wang et al., 2017; Lu et al., 2015). These references are now included in the manuscript.

Su, B., Huang, J. L., Zeng, X. L., Gao, C., and Jiang, T.: Impacts of climate change on streamflow in the upper Yangtze River basin, Clim. Change, 141, 533-546, https://doi.org/10.1007/s10584-016-1852-5, 2017.

Wang H., Sun F. B., Xia J., Liu W. B.: Impact of LUCC on stream flow based on the SWAT model over the Wei River basin on the Loess Plateau in China, Hydrol. Earth Syst. Sci., 21, 1929-1945, 2017 www.hydrol-earth-syst-sci.net/21/1929/2017/ doi:10.5194/hess-21-1929-2017

Lu Z. X., Zou, S. B., Qin Z. D., Yang, Y. G., Xiao, H. L., Wei Y. P., Zhang K., and Xie J. L.: Hydrologic Responses to Land Use Change in the Loess Plateau: Case Study in the Upper Fenhe River Watershed, Advances in Meteorology. 2015. 1-10. 10.1155/2015/676030.

Comment 11: *In section 4.1 and 4.3, while determining the trends, was statistical trend analysis applied? Or how were the trends determined? By only visual technique?*

Answer:

We combine the statistical and visual techniques to explore the trends presented in sections 4.1 and 4.3. We added detail values (shown in table 5), which are described in sections 4.1 and 4.3. In order to visualize the precipitation, temperature and simulated discharge, we presented trends in figure format (Fig. 3, Fig. 4 and Fig. 9).

Table 5 Mean values of temperature, precipitation and simulated discharge in different scenarios

		piControl scenario	Historical scenario	Future scenario			
				RCP2.6	RCP4.5	RCP6.0	RCP8.5
Temperature (℃)	1861-2005	6.40	6.53	-	-	-	-
	2006-2099	6.41	-	8.27	8.79	8.70	9.72
	2100-2299	6.43	-	8.38	10.48	-	19.94
Precipitation (mm)	1861-2005	821.8	805.7	-	-	-	-
	2006-2099	819.2	-	814.9	823.8	809.8	830.2
	2100-2299	835.7	-	854.2	841.0	-	790.4
Discharge (m^3s^{-1})	1861-2005	10578.0	10294.4	-	-	-	-
	2006-2099	11338.6	-	10784.6	10592.6	10224.6	10617.8
	2100-2299	11698.5	-	11859.2	11824.3	-	10279.2

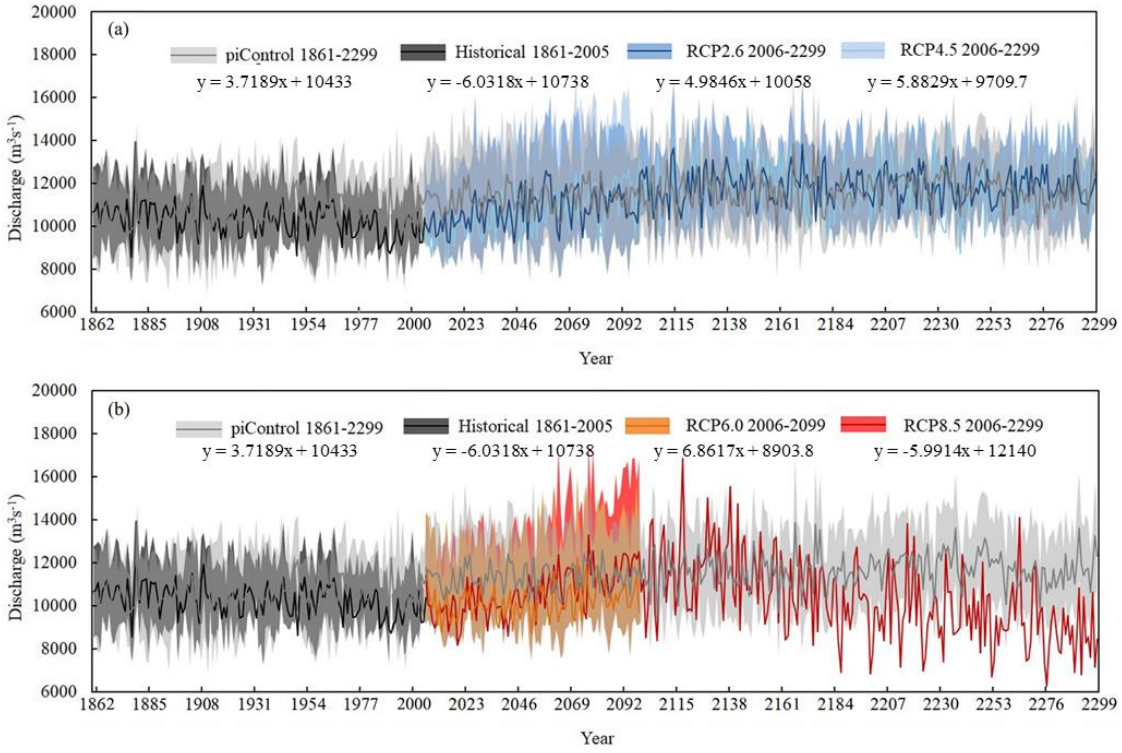

Figure 9 The annual mean discharge at the Cuntan station simulated by four hydrological models (HBV, SWAT, SWIM, and VIC) under the piControl scenario and scenarios with anthropogenic climate change effects (a-b)

N.B.: Because of taking up too many pages, we only include Fig. 9 here . See Fig. 3 and Fig. 4 in the revised paper.

Comment 12: *In section 4.2, please explain what the model performance threshold is. Is it for good performance? Please give reference/references for it (Table 4). In addition, please comment why SWIM and VIC models had lower performance in the validation period. Moreover, please provide Q90 results in Fig. 5 which shows the scatter plots. So, in this figure, the coefficient of determination (R2) of 4 hydrological models should be given for significance of the scatter plots. Likewise, WLS values of extreme conditions should be presented for the calibration period. For this section, finally, please show the mean annual evapotranspiration outputs of the other three models based on sub-basins in Fig. 7 and compare all of the models with GLEAM based on statistical and/or mathematical criteria. It is better to see the all models in comparison. Even further, VIC and GLEAM could be compared based on grid by means of a confusion matrix.*

Answer:

We have added the thresholds of acceptance in Table 6 and the references in Table 4 as follow:

"In this study, four criteria, the NSE, RSR, Pearson's correlation coefficient (r) and KGE, are applied to the daily discharge series to evaluate the performance of hydrological models (Krysanova et al., 2018; Table 4). Thresholds of acceptance of four criteria are derived from the references (Nash and Sutcliffe, 1970; Moriasi et al., 2007; Huang et al., 2012; King et al., 2012)."

Table 6 Performance of four hydrological models in the upper Yangtze River at the calibration period and the wet and dry validation periods

criterion	Thresholds of acceptance	calibration/validation	HBV	SWAT	SWIM	VIC
NSE	>=0.7	1979-1990	0.86	0.81	0.75	0.89
		1967-1978 (wet period)	0.86	0.79	0.7	0.88
		1991-2002 (dry period)	0.86	0.81	0.75	0.89
RSR	<=0.6	1979 - 1990	0.39	0.43	0.50	0.33
		1967-1978 (wet period)	0.38	0.46	0.55	0.34
		1991-2002 (dry period)	0.36	0.42	0.48	0.32
r	>=0.9	1979-1990	0.92	0.91	0.91	0.97
		1967-1978 (wet period)	0.92	0.90	0.89	0.96
		1991-2002 (dry period)	0.94	0.92	0.93	0.97
KGE	>=0.7	1979-1990	0.87	0.9	0.7	0.71
		1967-1978 (wet period)	0.90	0.88	0.65	0.69
		1991-2002 (dry period)	0.85	0.89	0.56	0.68

Table 4 Evaluation criteria for testing simulation capacity of hydrological models

Criterion	Formula	Range	Ideal value	Notation	Reference
Nash-Sutcliffe efficiency (NSE)	$1-\frac{\sum_{t=1}^{N}(Q_{s,t}-Q_{o,t})^2}{\sum_{t=1}^{N}(Q_{o,t}-\acute{Q}_o)^2}$	(-∞, 1)	1	Q_s: simulated discharge; Q_o: observed discharge; $\bar{Q}$； $\bar{Q}\acute{Q}_o$: mean of observed discharge; $\acute{Q}_s$: mean of simulated discharge; t: sequence of the discharge series; N: number of time steps; α: ratio between the standard deviations of the simulated and observed data; β: ratio between the mean simulated and mean observed discharge	(Nash and Sutcliffe, 1970)
Ratio of the root mean square error and the standard deviation of observation (RSR)	$\frac{\sqrt{\sum_{t=1}^{N}(Q_{o,t}-Q_{s,t})^2}}{\sqrt{\sum_{t=1}^{N}(Q_{o,t}-\acute{Q}_o)^2}}$	(0, +∞)	0		(Moriasi et al., 2007)
Pearson's correlation coefficient (r)	$\frac{\sum_{t=1}^{N}(Q_{s,t}-\acute{Q}_s)(Q_{o,t}-\acute{Q}_o)}{\sqrt{\sum_{t=1}^{N}(Q_{s,t}-\acute{Q}_s)^2}-\sqrt{\sum_{t=1}^{N}(Q_{o,t}-\acute{Q}_o}}$	(-1, 1)	1		(Huang et al., 2012)
Modified Kling -Gupta efficiency (KGE)	$1-\sqrt{(\alpha-1)^2+(\beta-1)^2+(r-1)^2}$	(-∞, 1)	1		(King et al., 2012)

The parameters in hydrological models are changed during the calibration process within ranges indicated in Table 4 and iterated continuously. The parameters are not adjusted during the validation period. This is the reason why some models had lower performance in the validation period compared to the calibration period.

We have added the Q10 and Q90 scatter plots with the coefficient of determination (R^2) in Fig.6.

N.B.: The previous version of Fig. 6 included only Q10. Now both Q10 and Q90 are included.

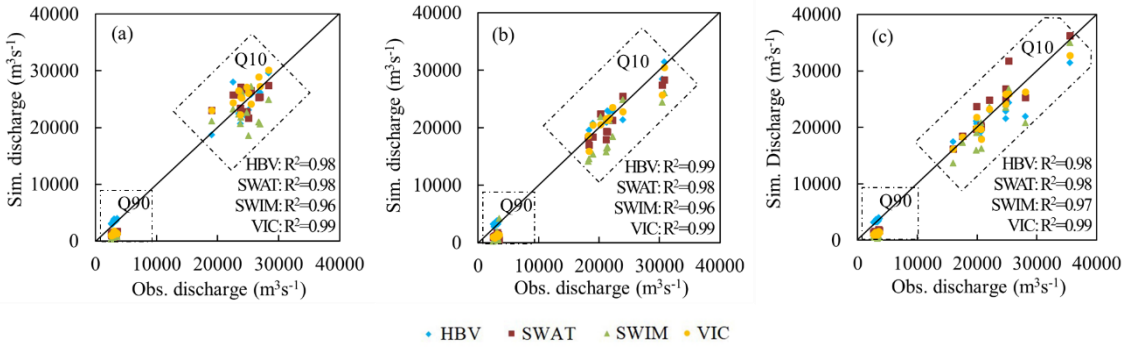

Figure 6 Comparison of the simulated and observed Q10, Q90 percentiles at the Cuntan station in the calibration period 1979 - 1990 (a) and validation period 1967 - 1978 (b) and 1991 - 2002 (c)

The annual evapotranspiration outputs of HBV, SWAT, SWIM, VIC are compared with GLEAM (0.25°×0.25°). The visual techniques are used to compare spatial distribution pattern of evapotranspiration. Besides, output of VIC is selected to set up a confusion matrix to compare with GLEAM evapotranspiration in gridded scale. The confusion matrix is obtained using 500 randomly selected pixel samples of VIC and GLEAM datasets. The kappa value, which is the result of confusion matrix, reaches 0.62, and indicating a substantial agreement of two datasets (the process is shown in the table below).

N.B.: Previous version showed the resample result from 0.25°×0.25° to 0.5°×0.5°. Now the results with original resolution are presented in the revised version.

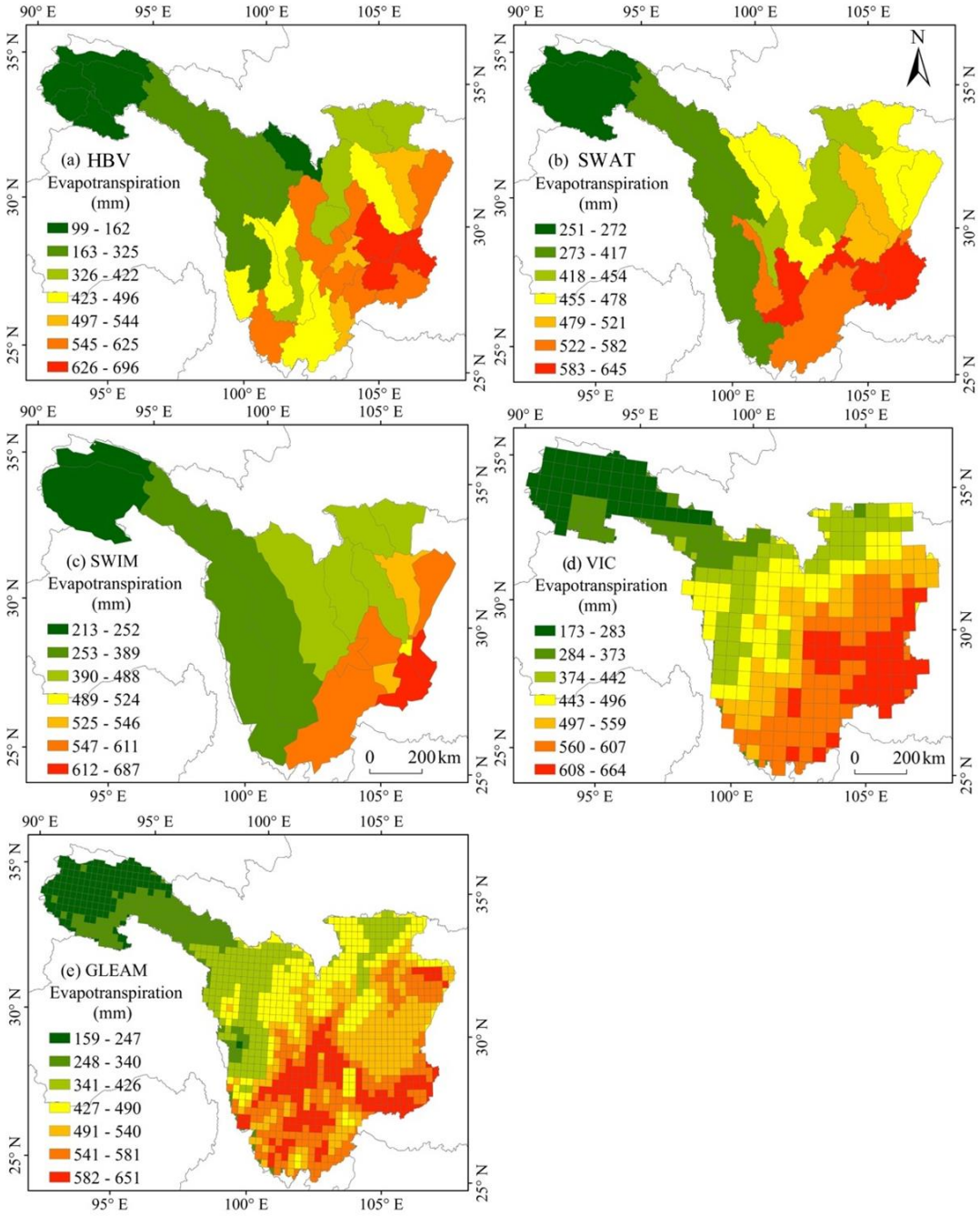

Figure 8 Spatial distribution of multi-year averaged annual evapotranspiration in the upper Yangtze River basin for 1986 - 2005: HBV output (a), SWAT output (b), VIC output (c), SWIM output (d) and GLEAM data(e)

Table of confusion matrix process of VIC and GLEAM (not shown in the revised paper)

ClassValue	159-247	248-340	341-426	427-490	491-540	541-581	582-651	Total	U_Accuracy	Kappa
171-283	50	19	0	0	0	0	0	69	0.72	0.00
284-373	2	32	8	0	0	0	0	42	0.76	0.00
374-442	0	3	55	15	2	4	0	79	0.70	0.00
443-496	0	0	10	54	10	4	2	80	0.68	0.00
497-559	0	0	1	12	37	16	0	66	0.56	0.00
560-607	0	0	0	4	14	56	16	90	0.62	0.00
608-664	0	0	0	3	7	11	52	74	0.70	0.00
Total	52	54	74	88	70	91	70	500	0.00	0.00
P_Accuracy	0.96	0.59	0.74	0.61	0.53	0.62	0.74	0.00	0.67	0.00
Kappa	0.00	0.00	0.00	0.00	0.00	0.00	0.00	0.00	0.00	**0.62**

Comment 13: *In competing interests section, please give information of author contribution for each author in favor of justice.*

Answer:

As suggested by reviewer, we added the author contribution (Page9) in the manuscript as follows: "Chao Gao, Buda Su, Qianyu Zha, Cai Chen and Gang Luo run the hydrological models. Chao Gao, Buda Su and Tong Jiang analysed results and draft the manuscript. Xiaofan Zeng, Jinlong Huang, Min Xiong and Liping Zhang assisted in the data processing. Valentina Krysanova provided guidance for the calibration/validation of the models and the description of results. All authors reviewed the resulting inventory and assisted with paper writing."

Comment 14: *In Fig. 1, please present DEM to get to know the basin better. And please specify how many grid cells are in the basin.*

Answer:

The same as for question 3, we added the DEM, and the 311 grids of climate models in the basin (Fig. 1).

Title of the Fig. 1 is changed to: Location of the Cuntan hydrological station, GCM grids, meteorological stations and spatial distribution of the land use and soil types in the upper Yangtze River basin"

Comment 15: *In titles of Fig. 2 and Fig. 3, "seasonal" expressions should be replaced with "monthly".*

Answer:

We have switched the "seasonal" to "monthly" in Fig. 3 and Fig. 4:

"Figure 3 Inter-annual (a) and long-term averaged monthly dynamics (b-d) of the surface air temperature in the upper Yangtze River basin: comparison of the piControl scenario with the anthropogenic climate change scenarios (periods: a: 1861 - 2299; b: 1861 - 2005; c: 2006 - 2099; and d: 2100 - 2299)

Figure 4 Inter-annual (a-b) and long-term averaged monthly dynamics (c-e) of precipitation in the upper Yangtze River basin: comparison of the piControl scenario with the anthropogenic climate change scenarios (periods: a: 1861-2299; b: 1861-2299; c: 1861 - 2005; d: 2006 - 2099; and e: 2100 - 2299)"

Comment 16: *Although the study is daily flow modeling, the graphical representation in Fig. 6 is given on monthly time scale since the application period is very long. If so, please express this.*

Answer:

We selected monthly time scale to show trend because the period is quite long.

Comment 17: *In Fig. 8, are the values mean outputs of hydrological models and GCMs (a-b)? And there is a noteworthy decreasing in discharge (d), why? Please comment. And why is "2100-2169" period not available (c-d)?*

Answer:

Fig.8 shows the simulated annual mean discharge averaged over four hydrological models and four GCMs.

The decrease of simulated discharge in 2170-2199 can be explained by trends of precipitation projected by GCMs, which show an increase trend in the 21st century but a decrease trend in the 22nd century.

There is no sense to compare only the long-term monthly means and average values for such a long period. Climate projections and hydrological impacts for the past and future periods can be analyzed for 30 y periods. Thus, we selected the periods of 2070-2099 and 2270-2299 to describe the average monthly discharge and statistical distribution of the daily maximum discharge:

"Similar to precipitation and temperature, average monthly discharge in 2070 - 2099 and 2270 - 2299 under both the piControl and RCP scenarios show single peak. Under RCP 4.5, a higher flood volume of August is projected in periods of 2070 - 2099 and 2270 - 2299 than the piControl scenario. Meanwhile, a higher volume in 2070 - 2099 but a lower in 2270 - 2299 under RCP8.5 is projected. Under RCP2.6, the flood volume of August is similar to piControl in both periods (Fig. 10a-b). The Generalized Logistic Distribution (GLD), which is the optimistic distribution by Kolmogorov - Smirnov goodness of fit test, is applied to describe the statistical distribution of the daily maximum discharge (represented by annual Q10) for 2070-2099 and 2270-2299. It is found that the return

level of daily maximum discharge under RCP2.6, RCP4.5, RCP6.0 and RCP8.5 are higher than piControl scenario in 2070 - 2099 (Fig. 10c). Under RCP 4.5, a higher average of return level of daily maximum discharge is projected in periods of 2070 - 2099 and 2270 - 2299 than the piControl scenario. For RCP8.5, the average of return level of daily maximum discharge is higher in 2070 - 2099 but lower in 2270 - 2299 than piControl scenario. Under RCP2.6, the average of return level of daily maximum discharge is similar to piControl scenario in both periods (Fig. 10c-d)"

> ***Comment 18:*** *In Table 4, it is interesting that the performance criteria are so close between the cal-val periods. Please comment what the reason.*

Answer:

Usually, a hydrological model has a certain stability when applied in the same watershed, and the criteria values in the validation period are lower than those in the calibration period but could be also close to them.

Technical Corrections

> ***Comment 19:*** *P3L6 and L7: "0.2 °C/10a" and "-11 mm/10a" → Please present as open.*

Answer:

Thank you for your advice. We have adjusted it.

> ***Comment 20:*** *P4L27: "(Moriasi et al., 2007)" must be placed in the end of the sentence.*

Answer:

We have moved the reference (Moriasi et al., 2007) to the end of sentence as follow:
"For evaluating daily hydrograph simulation, ratio of the root mean square error to the standard deviation of measured data (RSR) is recommended (Moriasi et al., 2007)"

> ***Comment 21:*** *P5 L21-L22 and P6 L2-L3: "seasonal" → "monthly".*

Answer:

Thank you for your advice. Revised as suggested.

> ***Comment 22:*** *P6 L27: "models could reproduce the monthly river flow …" → Please explain which one of "monthly modeling" or "daily modeling and transforming into monthly" was performed.*

Answer:

All four hydrological models simulated daily river flow, which was later transformed in the monthly river flow.

Comment 23: *P7 L13 and L14: "with the exception of RCP 6.0" → Please comment.*

Answer:

No projection has been done for 2170-2199 under RCP6.0 (see details in Table 1)

Table 1 Availability of climate scenarios from four GCMs for different periods

Climate scenario	CO_2 concentration	GFDL-ESM2M	HadGEM2-ES	IPSL-CM5A-LR	MIROC5
piControl scenario	286 ppm	1861-2099	1861-2299	1861-2299	1861-2299
Historical scenario	Recorded CO_2	1861-2005	1861-2005	1861-2005	1861-2005
Future scenario	RCP2.6	2006-2099	2006-2299	2006-2299	2006-2299
	RCP4.5	2006-2099	2006-2099	2006-2299	2006-2099
	RCP6.0	2006-2099	2006-2099	2006-2099	2006-2099
	RCP8.5	2006-2099	2006-2099	2006-2299	2006-2099

Comment 24: *P7 L14 and L15: "an increasing trend in the 21st century, turning into a decreasing trend in the 22nd century." → Why? Please explain considering the precipitation.*

Answer:

It related to the precipitation trend, which increases in the 21st century but decreases in the 22nd century, as explained before (response to Q16). More details are added in the revision to make it clear:

"The simulated discharge time series for 1861 - 2299 under the piControl scenario without anthropogenic climate change and scenarios with anthropogenic climate change effects are shown in Fig. 9a-b. Similar to precipitation trend, annual mean discharge at the Cuntan station shows no significant trend from 1861 to 2299 under the piControl scenario. In historical period, annual mean discharge has shown a slight decrease trend in 1861 - 2005. Under RCPs, annual mean discharge will be in a significant upward trend by the end of the 21st century with increasing variation in the upper Yangtze River. Annual mean discharge shows no significant change since 2100 under RCP2.6 and RCP4.5, but a rapid decline is projected under high emission RCP8.5 scenario in future (Fig. 9a-b, Table 5)"

Comment 25: *P7 L18: "11,517 m3s-1" → "11,517 m3s-1 (363.2 billion m3)". For comparison of observation value stated in the section of study area.*

Answer:

According to the simulation results outputted by four hydrological models, the mean annual discharge in the piControl scenario is 11,517 m^3s^{-1}(the number represent the scenario of PiControl spans more than 400 years since 1861 to 2299). The value mentioned in the study is the mean value of the observations in recent decades, which is far less than the piControl. It is no sense to compare the piControl result and observation data. We revised the manuscript as:

"Comparison of relative changes in mean annual discharge for 2070-2099 and 2270-2299 under RCPs with that of the piControl scenario is presented in Table 7. Relative to the piControl scenario, change of annual mean discharge will be -4.2 %, -1.1 %, -9.1 % and -0.7 % respectively, under RCP2.6, RCP4.5, RCP6.0 and RCP8.5, in 2070 - 2099. And the relative change of annual mean discharge will be 2.2 %, 2.6 % and -30.6 %, respectively, under RCP2.6, RCP4.5 and RCP8.5 in 2270 - 2299 (Table 7)."

Table 7 Relative changes in mean annual discharge, Q10 and Q90 in the periods 2070 - 2099 and 2270 - 2299 under the scenarios of anthropogenic climate change relative to the piControl scenario

Period	Scenarios	Relative change of mean discharge (%)	Relative change of Q10 (%)	Relative change of Q90 (%)	Standard deviation	Coefficient of variation
2070-2099	piControl	-	-	-	607.1	0.05
	RCP2.6	-4.2	-1.2	-5.4	681.1	0.06
	RCP4.5	-1.1	3.2	-10.9	997.1	0.09
	RCP6.0	-9.1	-3.5	-10.6	763.7	0.07
	RCP8.5	-0.7	4.3	-3.5	917.3	0.08
2270-2299	piControl	-	-	-	767.6	0.06
	RCP2.6	2.2	2.5	3.2	608.8	0.05
	RCP4.5	2.6	6.6	-2.3	1255.9	0.11
	RCP6.0	-	-	-	-	-
	RCP8.5	-30.6	-13.2	-50.4	1397.4	0.16

Comment 26: *P7 L23: "(except for RCP 4.5)" → Why? Please interpret.*

Answer:

Further evaluation needs to be done for some more specific reasons. In our opinion, it may be related to the Availability of time series (see details in Table 1). It contains data for 2006-2099 both for the RCPs and piControl. But there are different time series data of GCMs during the period of the 2100-2299, for example, for RCP2.6 (3 GCMs), RCP4.5 (only one, IPSL), RCP6.0 (none), RCP8.5 (2 GCMs). And now we divided 2006-2299 into 2006-2099 and 2100-2299 (page 7, line 4) to describe the relative changes in mean annual discharge for 2006-2099 and 2100-2299 under RCPs with that of the piControl scenario.

Table 1 Availability of climate scenarios from four GCMs for different periods

Climate scenario	CO_2 concentration	GFDL-ESM2M	HadGEM2-ES	IPSL-CM5A-LR	MIROC5
piControl	286 ppm	1861-2099	1861-2299	1861-2299	1861-2299
Historical	Recorded CO_2	1861-2005	1861-2005	1861-2005	1861-2005
Future	RCP2.6	2006-2099	2006-2299	2006-2299	2006-2299
	RCP4.5	2006-2099	2006-2099	2006-2299	2006-2099
	RCP6.0	2006-2099	2006-2099	2006-2099	2006-2099
	RCP8.5	2006-2099	2006-2099	2006-2299	2006-2099

Comment 27: *P8 L30: "For the calibration" → "For the calibration and the validation periods".*

Answer:

We corrected the statement and deleted the sentence "For the calibration and the validation periods".

"Four criteria, including the NSE, KGE, RSR and r, are used to evaluate the parameterization results. To assess the models' ability to satisfactorily simulate discharge under different climate conditions, hydrological models are validated both in dry and wet periods. Besides, evapotranspiration outputs by simulation process are compared with remote-sensing-based evapotranspiration from the GLEAM dataset to further validate performance of the models."

Comment 28: *P9 L1: "a cross-validation method" → Please give info. Leave-one-out or k-fold technique? If leave-one-out technique, it is problem of independence of validation dataset.*

Answer:

Here, the 'cross-validation' is not another technique but a method that considers evapotranspiration apart from discharge to test performance of hydrological model and improve the reliability of results.

"Four criteria, including the NSE, KGE, RSR and r, are used to evaluate the parameterization results. To assess the models' ability to satisfactorily simulate discharge under different climate conditions, hydrological models are validated both in dry and wet periods. Besides, evapotranspiration outputs by simulation process are compared with remote-sensing-based evapotranspiration from the GLEAM dataset to further validate performance of the models."

Comment 29: *P9 L6 and L7: "the simulated extreme peak values in the 1930s, 1950s and 1990s were also in good agreement with the historical documented records ...→Please add "except 1998 flood" for objectiveness and being non-manipulative. It is specified that the modeled peak flow is 36,000 m3/s (in P6 L20) and the observed value is 68,500 m3/s (in P4 L9) for the 1998 flood event.*

Answer:

Thank you for your vital advice. We mentioned in the paper that the peak flows of simulated discharge in 1930s, 1950s and 1990s were 64,300 m^3s-^{1}, 53,900 m^3s^{-1} and 60,700 m^3s^{-1}, respectively, deviating by less than 10 % from the recorded peaks, i.e., it means we compared the daily peak flows simulated by hydrological models and recorded peaks, rather than the Q10 results. Now, we reorganized the statement of this paper as follows:

"The four hydrological models can also properly simulate high flow and low flow represented by Q10 and Q90 in calibration and validation periods. For example, Q10 result illustrates that the several severe floods mentioned previously are reproduced quite well by the model simulations: the peak flows of simulated discharge were 64,300 m^3s^{-1}, 53,900 m^3s^{-1} and 60,700 m^3s^{-1}, respectively, in the 1930s, 1950s and 1990s, deviating by less than 10 % from the recorded peaks (Fig. 6)."

Comment 30: *The references in P12 L5 and P12 L8 must be replaced due to the alphabetical order.*

Answer:

Thanks for your suggestion. Revised as suggested.

Comment 31: *In accordance with the aim-scope of the journal, the dataset control process of the review is rather important case. For future reuse and reinterpretation, I checked the quality of the datasets which are available at the relevant web link. I think there is potential of the data being useful in the future but there is only simulated discharge file (xls) as time series. The observed data (discharge, precipitation, temperature, etc.), the data of GCMs (precipitation, temperature, etc. for pi and RCP scenarios), the evapotranspiration data of 4 hydrological models and GLEAM (as time series), the grid evapotranspiration data (GLEAM and VIC) and the other grid data used (DEM, soil and land use data) must be also presented for both reproducibility of scientific and usefulness of data. In addition, to perform tests for data quality, the above-mentioned data sets are necessary. The availability of these datasets is important for usefulness and completeness, too. And at the aim and scope web page of the journal, the expression of "each article should publish as much data as possible" supports the completion of deficiencies.*

Answer:

We will upload the simulated discharge file and evapotranspiration data, observed meteorological data including precipitation and temperature, etc. GCMs data, GLEAM evapotranspiration, 1990 land use, DEM at 90m resolution. Amongst, GCM data (precipitation, temperature, etc. for pi and RCP scenarios) were obtained from ISMIP project. The soil property data were obtained from the Harmonized World Soil Database of the Food and Agriculture Organization of the United Nations (http://www.fao.org/), and the spatial distribution of soil types (1:1,000,000) was taken from the Institute of Soil Science of the Chinese Academy of Sciences (CAS). A land use map (1:1,000,000) for 1990 was provided by the Data Center for Resource and Environmental Sciences of the CAS.

Best regards,

Chao Gao and co-authors

A 439-year simulated daily discharge dataset (1861-2299) for the upper Yangtze River, China

Chao Gao[1], Buda Su[2], Valentina Krysanova[3], Qianyu Zha[1], Cai Chen[1], Gang Luo[1], Xiaofan Zeng[4], Jinlong Huang[5], Min Xiong[6], Liping Zhang[7], Tong Jiang[5]

[1]Department of Geography & Spatial Information Techniques, Ningbo University, Ningbo, 315211, China;

[2]National Climate Centre, China Meteorological Administration, Beijing 100081, China;
[3]Potsdam Institute for Climate Impact Research, Potsdam, Germany;
[4]School of Hydropower and Information Engineering, Huazhong University of Science and Technology, Wuhan, 430074, China;
[5]Collaborative Innovation Center on Forecast and Evaluation of Meteorological Disasters, Institute for Disaster Risk Management (iDRM), School of Geographical Science, Nanjing University of Information Science & Technology, Nanjing 210044, China;
[6]Bureau of Hydrology, Changjiang River Water Resources Commission, Wuhan, 430010, China;
[7]State Key Laboratory of Water Resources and Hydropower Engineering Science, Wuhan University, Wuhan, 430072, China

Correspondence to: Tong Jiang (jiangtong@nuist.edu.cn)

Abstract. The outputs of four Global Climate Models (GFDL-ESM2M, HadGEM2-ES, IPSL-CM5A-LR and MIROC5), which were statistically downscaled and bias corrected, were used to drive four hydrological models (HBV, SWAT, SWIM and VIC) to simulate the daily discharge at the Cuntan hydrological station in the upper Yangtze River from 1861 to 2299. As the performances of hydrological models in various climate conditions could be different, the models were first calibrated in the period from 1979 to 1990. Then, the models were validated in the comparatively wet period, 1967 - 1978, and in the comparatively dry period, 1991 - 2002. A multi-objective automatic calibration programme using a univariate search technique was applied to find the optimal parameter set~~s~~ for each of the four hydrological models. The Nash-Sutcliffe efficiency (NSE) of daily discharge and the weighted least squares function (WLS) of extreme discharge events, represented by high flow (Q10) and low flow (Q90), were included in the objective functions of the parameterization process. In addition, the simulated evapotranspiration results were compared with ~~evapotranspiration data from the~~ GLEAM evapotranspiration data ~~project~~ for the upper Yangtze basin. For evaluating the performances of the hydrological models, the NSE, modified Kling-Gupta efficiency (KGE), ratio of the root mean square error to the standard deviation of the measured data (RSR) and Pearson's correlation coefficient (r) were used. The four hydrological models ~~showed good performance in the calibration and validation periods~~ reach satisfactory simulation results

both in the calibration and validation periods. In this study, the daily ~~runoff~~ discharge ~~was~~ is simulated for the upper Yangtze River under the preindustrial control (piControl) scenario without anthropogenic climate change~~,~~ from 1861 - 2299, and for the historical period 1861 - 2005~~,~~ and for 2006 to 2299 under the RCP2.6, RCP4.5, RCP6.0 and RCP8.5 scenarios ~~in the period from 2006 to 2299~~. The long-term daily discharge datasets ~~for the upper Yangtze River provide streamflow trends in the future and clues regarding to what extent human-induced climate change could impact streamflow.~~ can be used in the international context and water management, e.g. in the framework of Inter-Sectoral Impact Model Intercomparison Project (ISIMIP) by providing clue to what extent human-induced climate change could impact streamflow and streamflow trend in future. The datasets are available at the https://doi.org/10.4121/uuid:8658b22a-8f98-4043-9f8f-d77684d58cbc (Gao et al., 2019).

1 Introduction

~~With the progress of industrialization, global warming has been escalating. Global warming~~ Global warming is the long-term rise in average temperature of the earth's climate system. Warming temperature alters global water circulation processes and could significantly influence the sustainability of the ~~social~~ society and economy (Jung et al., 2011). The variation in water resource availability in the context of global warming ~~has become the focus of hydrological research~~ is acknowledged as a focus of many international research projects (~~Su et al., 2015;~~ Stagl et al., 2016; Raman et al., 2018; Maisa et al., 2019). The long-term accurate (as much as possible) daily ~~runoff sequences~~ discharge time series are crucial for ~~an~~ in-depth understanding of the changes in ~~global water resources~~ in streamflow, and they are needed for subsequent ~~research~~ climate change impact studies. However, ~~runoff is commonly monitored for only~~ discharge is monitored usually only for short observational periods in most river basins.

~~To date, the sedimentological method, hydrological field survey method, and recorded historical documents have been used to develop long-term runoff series.~~ For generation of the long-term streamflow series, many data mining techniques including the sedimentological method, the hydrological field survey method, and the documentary analysis method can be applied (Longfield et al., 2018). ~~However~~ Nevertheless, ~~the~~ low temporal resolution and insufficient ~~estimation~~ accuracy of these ~~methods and resources~~ estimations can hardly meet the demands of practical and research applications. Instead, the observed climatic variables and the outputs of ~~Global Climate Models (GCMs) and Regional Climate~~

~~Models (RCMs)~~ climate models have often been used to drive hydrological models to evaluate changes in ~~runoff~~ streamflow in the context of climate change (Braud et al., 2010; Chen et al., 2017; Su et al., 2017; Dahl, 2018; Seneviratne et al., 2018). ~~However~~ But there is a lack of research on the quantitative estimation of long-term ~~runoff~~ streamflow for period~~s~~ longer than 400 years~~, especially~~ under scenarios with and without anthropogenic climate change (Meaurio, 2017).

The Yangtze River is the longest river in China. It originates ~~on~~ from the Tibetan Plateau and enters the East China Sea after flowing through 11 provinces. With a large topographic gradient and substantial ~~mean annual~~ water supply of approximately 10,000 m^3s^{-1} on the average, the upper Yangtze River is rich in hydropower resources, but ~~is~~ subject~~ed~~ to destructive flash floods. The Yangtze River basin has the longest hydrological observations in China. ~~with~~ Data provided by the Cuntan hydrological station, which started operating in 1939, ~~This data availability~~ facilitates hydro-meteorological studies in the instrumental period (Su et al., 2008; Wang et al., 2008; Su et al., 2017). As changes in ~~runoff~~ streamflow at the Cuntan station directly influence the ~~water supply of~~ inflow to the Three Gorges Reservoir, establishing ~~a~~ long-term ~~runoff~~ discharge ~~time~~ series at the Cuntan station ~~could~~ can support ~~the development of hydraulic management strategies in the upper Yangtze Rive~~r. effective management of hydraulic projects. Besides, the longer discharge series can also provide a possibility to explore impacts of anthropogenic climate change on hydrology for international climate change research community. Therefore, ~~the main aim of this study was to~~ we simulate~~d~~ daily discharge at the Cuntan hydrological station in the upper Yangtze River in the period ~~from~~ in the period 1861 - 2299 using available climate model outputs. The outputs of four downscaled GCMs (GFDL-ESM2M, HadGEM2-ES, IPSL-CM5A-LR, and MIROC5) are utilized to drive ~~and~~ four hydrological models (HBV, SWAT, SWIM and VIC) ~~were utilized~~ to simulate ~~runoff~~ discharge at the Cuntan station. The climate forcing comprised (a) the scenarios with anthropogenic climate change for the period 1861 - 2299, which ~~was~~ is subdivided into the historical period (1861 - 2005) and the future period (2006 - 2299) under different Representative Concentration Pathway (RCP) scenarios, and (b) the preindustrial control (piControl) scenario ~~without human-induced climate change~~ for the period 1861 - 2299, which ~~was~~ is used as a reference to detect the influence of anthropogenic climate change on ~~discharge~~ streamflow in the upper Yangtze River.

2 Study Area

~~With a catchment area of approximately 860,000 km^2, the mean annual runoff at the Cuntan hydrological station (29 ° 37 ′ N, 106 ° 36 ′ E) in the upper Yangtze River is 352.7 billion m^3, and the maximum peak discharge is 73,800 m^{3}s^{-1} (in 1945) for the period of instrumental measurements beginning in 1939. Influenced by the East Asian subtropical monsoon and a complex topography, the annual mean temperature exhibited an obvious increasing trend in the upper Yangtze from 11.4 °C (1950s) to 12.4 °C (2010s), with a slope of approximately 0.2 °C / 10 a. The annual precipitation decreased from 900 mm (1950s) to 845 mm (2010s), with a slope of -11 mm / 10 a.~~

The catchment area of the Cuntan hydrological station (29 ° 37 ′ N, 106 ° 36 ′ E) in the upper Yangtze River is approximately 860,000 km2, and 352.7 billion m3 water is flowing through this point annually with average discharge of 109,34 m3s-1 in the period of instrumental measurements beginning in 1939. Location of the Cuntan hydrological station, 311 GCM grids, meteorological stations and spatial distribution of the land use and soil types in the upper Yangtze River basin are shown in Fig. 1. Prairie grassland and acid purple soil are the most widespread of land use and soil type in the upper Yangtze River basin. The upper Yangtze River have complex geomorphic types and broken topography. Mountains and plateaus account for most of the region, hills and plains are few. Influenced by the East Asia subtropical monsoon and a complex topography, climate varies across the basin with annual air temperature and precipitation being high in the southeast but low in the northwest headstream region. According to observational data, the areal averaged annual mean temperature and precipitation are 12.3 °C and 1018 mm, respectively, during 1961 - 2017 in the upper Yangtze River basin.

3 Data and Methods

3.1 Climate scenarios

The outputs of the GCMs (GFDL-ESM2M, HadGEM2-ES, IPSL-CM5A-LR, and MIROC5) were statistically downscaled and bias corrected on a regular 0.5 × 0.5 ° resolution grid using a first-order conservative remapping scheme (Frieler et al., 2017; Lange, 2018). The GFDL model was developed by the Geophysical Fluid Dynamics Laboratory, Princeton University, USA, and all its integrations (approximately 100 in total), including GFDL-ESM2M and GFDL-ESM2G, were completed for the Coupled Model Intercomparison Project Phase 5 (CMIP5) protocol (Taylor et al., 2012). HadGEM2-ES is a coupled earth system model that was developed by the Met Office Hadley Centre, UK, for the CMIP5 centennial simulations (Jones et al., 2011). The IPSL-CM5A-LR model was developed by the Institute Pierre

Simon Laplace, France, and the model was built around a physical core that includes atmosphere, land surface, ocean and sea ice components (Dufresne et al., 2013). MIROC5 is a new version of the atmosphere-ocean GCM that was developed by the Japanese research community (Watanabe et al., 2010). ~~Due to a~~ Lack of long-term homogeneous observational data and existing of ~~the~~ confounding influence ~~of~~ from socioeconomic drivers, make GCM simulations rarely cover the preindustrial period. In this study, ~~the simulated~~ climate ~~conditions~~ simulations include a piControl scenario, representing ~~a preindustrial climate with a~~ a climate with natural variability under stable CO_2 concentration of 286 ppm, a historical scenario, representing the historical CO_2 concentration, and future RCP scenarios, representing various future CO_2 concentration pathways. The availability of climate scenarios for the different periods is shown in Table 1 (see also Frieler et al., 2017). Note that not all simulations ~~are available after 2099: from three models for RCP2.6, only from IPSL for RCP4.5 and RCP8.5, and no simulations for RCP6.0~~ cover 22nd and 23rd century. Data after 2099 are available from three models under RCP2.6, only from IPSL under RCP4.5 and RCP8.5, but no simulations under RCP6.0.

3.2 Observed meteorological and hydrological data

The observed daily meteorological data from 1951 - 2017 from 189 ground-based stations in the upper Yangtze River used in this study were quality controlled by considering changes in instrument type, station relocations, and trace biases at the National Meteorological Information Center of the China Meteorological Administration (Ren et al., 2010), which was inputted into the hydrological models by spatial interpolation. During 1951 - 2017, annual precipitation shows a decreasing trend, with multi-year average of 935 mm, and annual mean temperature has shown a positive trend with multi-year average of 10.5 °C. ~~The daily discharge data for the period 1939 – 2012 at the Cuntan station in the upper Yangtze River were derived from the China Hydrological Year book – Yangtze. Data from 1967 – 2002 were used for calibration and validation of the four hydrological models.~~ The daily discharge record at the Cuntan station in the upper Yangtze River is available for 1970 - 1999 from the China Hydrological Yearbook - Yangtze. The rest of daily record for periods 1939 - 1969 and 2000 - 2012 is collected from the Changjiang Water Resources Commission, Ministry of Water Resources in China.

~~With large variations in seasonal and interannual precipitation, the Yangtze River is prone to flooding. Disastrous flood events that occurred in 1870, 1931, 1954 and 1998 should be mentioned. In 1870, the most severe flood since 1153 occurred in the upper Yangtze River, with a flood peak at the Yichang~~

~~station (downstream of the Cuntan station) of approximately 100,500 m^3s^{-1}. The peak flows at the Cuntan and Yichang stations reached 63,600 m^3s^{-1} and 64,600 m^3s^{-1}, respectively, during the 1931 flood event and 52,200 m^3s^{-1} and 66,800 m^3s^{-1}, respectively, during the 1954 flood event. In 1998, the strongest flood of the 20th century occurred in the Yangtze River, and the peak flow at the Cuntan station reached 68,500 m^3s^{-1}.~~

The Yangtze River is prone to be flooded because of large inter- and inner-annual variations of precipitation. The most severe flood that can be tracked in the upper Yangtze River occurred in 1870, with a flood peak of approximately 100,500 m3s-1 at the Yichang station located downstream of the Cuntan station (Changjiang Water Resources Commission, 2002). The peak flows reached 63,600 m3s-1 and 64,600 m3s-1, respectively, at the Cuntan station and the Yichang station during the 1931 flood, and 52,200 m3s-1 and 66,800 m3s-1, respectively, during the 1954 flood (Hu and Luo, 1992; Luo and Le, 1996). During the strongest flood of the 20th century in the Yangtze River, the peak flow at the Cuntan station reached 68,500 m3s-1 in 1998 (Changjiang Water Resources Commission, 2002).

3.3 GLEAM evapotranspiration data

~~In addition to river discharge data,~~ Evapotranspiration data from the Global Land Evaporation Amsterdam Model (GLEAM) for ~~the period~~ 1986 - 2005 that were released by the University of Bristol (Miralles et al., 2011) ~~were~~ are used in our study to cross-check the performances of the hydrological models by means of the geographic information system (GIS) tools. ~~GLEAM is comprised of four mutually connected units: the Gash interception module, soil module, stress module, and Priestley-Taylor module. The remote sensing data were assimilated to obtain monthly evapotranspiration with a spatial resolution of 0.25°.~~ The GLEAM data was generated based on a variety of satellite-sensor products at monthly scale with a spatial resolution of 0.25°. The spatial distributions of simulated evapotranspiration with that from GLEAM are compared by GIS techniques, and kappa value of confusion matrix is also applied to evaluate the accuracy of simulated evapotranspiration (taking VIC output as an example) by refer to GLEAM.

3.4 Hydrological models and parameterization

Four hydrological models, HBV (Bergstrom et al., 1973), SWAT (Arnold et al., 1998), SWIM (Krysanova et al., 2005) and VIC (Liang et al., 1994), ~~were used to simulate river discharge at the Cuntan hydrological station.~~ are used to simulate river discharge at the Cuntan hydrological station, and a flowchart of the hydrological modelling process is shown in Fig. 2. A brief introduction to these four hydrological models is given in Table 2 (see also Hattermann et al., 2017).

~~3.5 Calibration and validation methods~~

~~A~~ The univariate search technique, which can evaluate the informativeness of each feature individually, ~~was~~ is used to calibrate the parameters ~~(Lai et al., 2006)~~. The objective functions include~~d~~ the Nash-Sutcliffe efficiency (NSE) of daily discharge (Nash and Sutcliffe, 1970) and the weighted least squares function (WLS) of high flow (Q10) and low flow (Q90). To achieve the maximum NSE and minimum ~~difference~~ gap between the observed and simulated ~~extremes~~, ~~the parameter values were changed more than 2,000 times within the ranges of the valid parameter scope.~~ parameterization processes are iterated over 2,000 times within the ranges of the valid parameter scopes in Table 3 (Lai et al., 2006).

For evaluating daily hydrograph simulations ~~(Moriasi et al., 2007)~~, ~~the~~ ratio of the root mean square error to the standard deviation of measured data (RSR) is recommended (Moriasi et al., 2007). In addition, the Kling-Gupta efficiency (KGE) was developed to provide diagnostic insights into the model performance by decomposing the NSE into three components: correlation, bias and variability (Gupta et al., 2009). In this study, four criteria, the NSE, RSR, Pearson's correlation coefficient (r) and KGE, ~~were~~ are applied to the daily time series to evaluate the performances of the hydrological models (~~Table 3~~ Krysanova et al., 2018; Table 4) .Thresholds of acceptance of four criteria are derived from the references (Nash and Sutcliffe, 1970; Moriasi et al., 2007; Huang et al., 2012; King et al., 2012).

.

~~3.6~~ 3.5 Geospatial information

A digital elevation model (DEM) with a resolution of 90 m from the Shuttle Radar Topography Mission database was used in this study. The soil property data were obtained from the Harmonized World Soil Database of the Food and Agriculture Organization of the United Nations (http://www.fao.org/), and the spatial distribution of soil types (1:1,000,000) ~~was~~ is taken from the Institute of Soil Science of the Chinese Academy of Sciences (CAS). A land use map (1:1,000,000) ~~for 1990 was~~ from ~~provided by~~ the Data Center for Resource and Environmental Sciences ~~of the CAS~~, ~~and this land use map was applied in the piControl, historical and RCP scenario periods (see discussion in Section 5).~~ CAS is applied for all hydrological runs under various climate conditions including the piControl, the historical and the RCP scenarios.

4 Results

4.1 Climate change in the upper Yangtze basin

~~Compared to that in the piControl scenario, the annual mean temperature in the historical period, 1861 - 2005, was slightly higher until the 1980s and showed a notable increase in the period 1986 – 2005 (Fig. 2) according to the ensemble mean of four GCMs. The annual mean temperature in 1986 – 2005 was 0.49 °C higher than that in the period 1861 – 1900 in the upper Yangtze basin, which was lower than the global average of 0.61 °C in the same period. Compared to the piControl scenario, under the RCP scenarios, the annual mean temperature was projected to increase significantly in the 21st century, by 1.1 - 6.9 °C. According to climate model projections, after 2100, the surface air temperature will remain stable under RCP2.6 and increase only slightly under RCP4.5, but a significant increase in temperature will continue under the RCP8.5 scenario, with an increase up to 13.5 °C compared to that in the piControl scenario (Fig. 2a).~~ According to ensemble mean of four GCMs, annual mean temperature in the upper Yangtze River basin in the period 1986 - 2005 is 0.49 °C higher than that in the period 1861 - 1900, the increase is lower than the global average of 0.61 °C in the same period. Compared to the piControl scenario, annual mean temperature is projected to increase significantly in the 21st century, by 1.85 ~ 3.31 °C under RCPs. After 2100, surface air temperature will remain stable under RCP2.6 and increase only slightly under RCP4.5, but a significant increase in temperature will continue under RCP8.5, with an increase up to 13.5 °C by 2299 compared to the piControl scenario (Fig. 3a, Table 5). The visible abruption ~~changes~~ in temperature in the year 2100 under RCP4.5 and RCP8.5 in ~~Fig. 2a~~ Fig. 3a are due to the fact that only the IPSL model runs were available after 2100 for these scenarios.

The long-term average ~~seasonal~~ monthly dynamics of temperature ~~were represented by~~ show a single-peak curve, ~~and~~ with July is the hottest month ~~was the month with the highest temperature under both the RCP scenarios and the piControl scenario~~. In the period 1861-2005, the ~~seasonal~~ inner-annual distribution pattern~~s~~ of temperature ~~were~~ is very similar for the piControl and the historical scenarios (Fig. 3b) ~~two scenarios, the piControl and historical scenarios (Fig. 2b)~~. However, differences in the monthly temperatures between the RCP scenarios and piControl scenario become apparent with time (~~Fig. 2c-d~~ Fig. 3c-d). Taking the temperature in July as an example, ~~the~~ differences between the two scenarios ~~were~~ are approximately 1.9 ~ 3.2 °C in the 21st century ~~and~~ but will enlarge to 1.7 ~ 12 °C in the period 2100 - 2299 ~~(Fig. 2c-d).~~

Compared with ~~the~~ precipitation ~~in the~~ under piControl scenario, which ~~had~~ has no monotonic trend, ~~the annual precipitation in the historical scenario showed a negative trend in the upper Yangtze basin, with an obvious decrease in the period 1986 - 2005 of approximately 7 % (60 mm). Under the RCP scenarios, the annual precipitation was projected to increase in the 21st century by up to 25.4 % compared to the precipitation simulated in the piControl scenario. The increase in precipitation tends to be stable, but the variation amplifies beginning in 2100. Especially under the RCP8.5 scenario, a wide range of fluctuations was projected with a variance as high as 86.1, which is 60.5 % higher than that in the piControl scenario (Fig. 3a).~~ annual precipitation is approximately 2 % (16 mm) less in 1861 - 2005 under historical scenario. With relative to the piControl scenario, changes of annual precipitation will be -1.2% ~ 1.3 % in the 21st century under RCPs, and will be 0.6 %~ 2.2 % in the 2100 - 2299 under RCP 2.6 and 4.5. Under RCP8.5, relative change of annual precipitation is -5.7 % and a wide range of fluctuations is projected with a variance as high as 94.3 in 2100 - 2299, which is 63.2 % higher than the piControl scenario (Fig. 4a-b, Table 5).

The long-term average ~~seasonal~~ monthly precipitation ~~was represented by~~ shows a single-peak curve, with ~~the~~ precipitation highest in July and the lowest ~~precipitation~~ in December and January. The differences in the long-term average ~~seasonal~~ monthly precipitation under the RCPs ~~scenarios~~ and the piControl scenario ~~were~~ are projected to ~~be~~ grow from -1.9 ~ 1.3 % before 2100 ~~but would grow~~ to -5.4 - 2.2 % in the period 2100 - 2299 (~~Fig. 3b-d~~ Fig. 4c-e).

4.2 Calibration and validation of the hydrological models

Previous study found that 1986/1987 was a change-point in the observational period for south China, with more obvious increase of temperature and decrease of precipitation since then (Thomas et al., 2012). ~~Fig. 4~~ Fig. 5 shows ~~the~~ that observed annual precipitation and runoff ~~observed~~ depth in the upper Yangtze basin in the period 1951 - 1986 are ~~1951 - 2012. The mean observed precipitation and runoff depth were~~ approximately 965 mm and 437 mm, respectively, ~~in the period 1951 - 1986~~ and decreased by 7 % and 5 % to 895 mm and 415 mm, respectively, in the period 1987 - 2012. ~~As shown in Fig. 4, 1986/1987 could be considered a turning point; the climate conditions become drier after 1987.~~ Therefore, the period 1979 - 1990, which included ~~years with~~ both comparatively wet and dry spells, ~~was~~ is chosen as the calibration period. ~~Then~~ Subsequently, ~~the~~ hydrological models ~~were~~ are validated in two periods without changing the parameters ~~found~~ set during the calibration: the wet spell~~,~~ 1967 - 1978, and the dry spell~~,~~

1991 - 2002.

Based on the NSE, RSR and r values, all four hydrological models performed quite well in both the calibration and validation periods for the simulations of daily discharge at the Cuntan station. In particular, the NSE values of all models exceeded 0.75 in the calibration period and 0.7 in the validation periods (~~Table 4~~ Table 6). The KGE values ~~were~~ are above the threshold in the calibration period for all models~~,~~ but ~~the values were~~ slightly lower in the validation period for the SWIM and VIC models.The four hydrological models ~~could~~ can also properly simulate the high flow~~s~~ represented by Q10 ~~(Fig. 5)~~ and Q90 in calibration and validation periods. ~~In addition, several of the severe observed floods that were mentioned previously were reproduced quite well by the simulated data, namely: extreme flood event of approximately 36,000 m^3s^{-1} (Fig. 5c) occurred in 1998 during the dry period, and extreme flood event of approximately 32,000 m^3s^{-1} (Fig. 5b) occurred in 1974 during the wet period.~~ For example, Q10 result illustrates that the several severe floods mentioned previously are reproduced quite well by the model simulations: the peak flows of simulated discharge ~~in the 1930s, 1950s and 1990s~~ were 64,300 m^3s^{-1}, 53,900 m^3s^{-1} and 60,700 m^3s^{-1}, respectively, in the 1930s, 1950s and 1990s, deviating by less than 10 % from the recorded peaks (Fig. 6).

To further validate the hydrological models, ~~the~~ discharge simulated in another thirty-year historical period (1939 - 1968) ~~was~~ is compared with the observed data ~~on the monthly scale~~ (~~Fig. 6~~ Fig. 7). It is ~~visible~~ found that there are systematic underestimations of streamflow by SWAT, SWIM and VIC ~~underestimate low flow, and high flow was underestimated in some of the wet years by all hydrological models.~~ But, all four hydrological models ~~could~~ can reproduce the monthly dynamics of river flow quite satisfactorily, with NSE values of 0.79 ~ 0.84 and *r* values of 0.91 ~ 0.92.

In addition, ~~the~~ evapotranspiration outputs of ~~the four hydrological models were~~ HBV, SWAT, SWIM, VIC are compared with the GLEAM evapotranspiration data ~~output~~ (see Section 3.3) in the period 1986 - 2005. The long-term average annual evapotranspiration simulated by the four hydrological models for the upper Yangtze basin ~~was~~ is ~~477 mm (range: 426 - 523 mm), which is consistent with the results from GLEAM (466 mm)~~ 442 mm, 487 mm, 484 mm, 466 mm, respectively, quite close to the result from GLEAM (452 mm). The spatial patterns of the gridded evapotranspiration outputs of the HBV, SWAT, SWIM, VIC model and GLEAM ~~are similar~~ all show low values in the northwest but high values in the southeast of the upper Yangtze River basin (~~Fig. 7~~ Fig. 8). ~~both models show low values in the north-western region but high values in the south-eastern region of the upper Yangtze basin. For the other three~~

~~models, which have spatial disaggregation into sub-basins and not in grid cells, the comparison of spatial patterns of evapotranspiration with the GLEAM output is not shown.~~ Furthermore, a matrix consisting of 500 randomly selected pixels from simulated evapotranspiration by VIC and corresponding GLEAM grids is set up to get the kappa value. The deduced kappa value of 0.62 indicates a substantial agreement of two date sources.

4.3 Simulation of daily discharge from 1861 - 2299

The simulated discharge time series for 1861 - 2299 under the piControl without anthropogenic climate change and scenarios with anthropogenic climate change effects are shown in Fig. 9a-b. ~~scenario and scenarios with anthropogenic climate change effects are plotted for the whole period 1861 - 2299 in Fig. 8a-b. In the period 1861 - 2005, the annual mean discharge at the Cuntan station had a slightly decreasing trend, which is similar to the precipitation trend (Fig. 3), which became visible in the late 20th century.~~ Similar to precipitation trend, annual mean discharge at the Cuntan station shows no significant trend from 1861 to 2299 under the piControl scenario. In historical period, annual mean discharge has shown a slight decrease trend in 1861 - 2005. ~~-~~Under the RCPs ~~scenarios~~, ~~the~~ annual mean discharge will be in a significant upward trend ~~in the upper Yangtze River shows a significant positive trend until 2100, with increasing variation~~ by the end of the 21st century with increasing variation in the upper Yangtze River~~. Beginning in 2100, the~~ annual mean discharge ~~has~~ shows no significant changes since 2100 under RCP2.6 and RCP4.5, but a rapid decline ~~in discharge~~ is projected under the RCP8.5 scenario in future (~~driven by the IPCL model only~~ Fig. 9a-b, Table 5).

Comparison of relative changes in mean annual discharge for 2006-2099 and 2100-2299 under RCPs with that of the piControl scenario is presented in Table 7. Relative to the piControl scenario, change of annual mean discharge will be -5.1 %, -7.0 %, -10.9 % and -6.8 % respectively, under RCP2.6, RCP4.5, RCP6.0 and RCP8.5, in 2006 - 2099. And the relative change of annual mean discharge will be 1.4 %, 1.1 % and -13.8 %, respectively, under RCP2.6, RCP4.5 and RCP8.5 in 2100 - 2299 (Table 7).

Under RCP2.6, RCP4.5 and RCP6.0, Q10 and Q90 discharge will be lower than that under the piControl scenario in 2006 - 2099. The relative changes of Q10 will be 1.4% higher but that of Q90 will be -12.6% lower under RCP8.5 than that under the piControl scenario in 2006 - 2099.

In 2100 - 2299, a higher Q10 discharge is projected under RCP2.6 and RCP4.5 than the piControl scenario. Meanwhile, a higher Q90 discharge under RCP2.6 but a lower Q90 discharge under RCP4.5 is projected. But the relative changes of Q10 and Q90 discharge will reach - 5.5 % and - 34.2 % due to the rapid declining of discharge under RCP8.5 in 2100 - 2299. The results indicate there will be more extreme hydrological events in the long run, especially under RCP8.5.

Similar to precipitation and temperature, average monthly discharge in 2070 - 2099 and 2270 - 2299 under both the piControl and RCP scenarios show single peak. Under RCP 4.5, a higher flood volume of

August is projected in periods of 2070 - 2099 and 2270 - 2299 than the piControl scenario. Meanwhile, a higher volume in 2070 - 2099 but a lower in 2270 - 2299 under RCP8.5 is projected. Under RCP2.6, the flood volume of August is similar to piControl in both periods (Fig. 10a-b). The Generalized Logistic Distribution (GLD), which is the optimistic distribution by Kolmogorov - Smirnov goodness of fit test, is applied to describe the statistical distribution of the daily maximum discharge (represented by annual Q10) for 2070-2099 and 2270-2299. It is found that the return level of daily maximum discharge under RCP2.6, RCP4.5, RCP6.0 and RCP8.5 are higher than piControl scenario in 2070 - 2099 (Fig. 10c). Under RCP 4.5, a higher average of return level of daily maximum discharge is projected in periods of 2070 - 2099 and 2270 - 2299 than the piControl scenario. For RCP8.5, the average of return level of daily maximum discharge is higher in 2070 - 2099 but lower in 2270 - 2299 than piControl scenario. Under RCP2.6, the average of return level of daily maximum discharge is similar to piControl scenario in both periods (Fig. 10c-d).

~~Higher return levels of daily maximum discharge were projected in the period 2070 – 2099 compared to those in the period 2170 – 2199 (Fig. 8c-d). Generally, the higher the emission scenario, the larger the return level is, with the exception of RCP6.0. When the model projections are taken as a whole, high discharge in the upper Yangtze River shows an increasing trend in the 21st century, turning into a decreasing trend in the 22nd century.~~

~~We also compared the changes under the climate warming scenarios in the whole future period 2006 – 2299 to those in the piControl scenario. According to the simulation results of the four hydrological models, the mean annual discharge in the piControl scenario is 11,517 m^3s^{-1}. Relative to that in the piControl scenario, the mean discharge is projected to decrease by 1.7–13.3 % under the RCP scenarios in the period 2006 – 2299 (see Table 5). This result indicates that anthropogenic climate change will induce a decrease in discharge in the upper Yangtze River, and the decrease would be larger under the higher RCP scenarios.~~

~~Regarding extremes, the Q90 discharge was projected to be lower under all RCP scenarios compared to that in the piControl scenario. Additionally, the Q10 discharge would also be slightly lower under the three RCP scenarios (except for RCP4.5) in the period 2006 – 2099 (Table 5), indicating an alleviation of flood risks but an aggravation of droughts in the future under global warming.~~

~~Regarding discharge variation, both the standard deviation and the coefficient of variation are higher under the RCP scenarios than under the piControl scenario (Table 5), which means that the discharge variation range would increase with the intensification of human-induced climate change.~~

4.4 Data availability

The current study ~~produced~~ generates ~~the~~ daily discharge time series for the upper Yangtze River at the ~~(~~Cuntan ~~gauge~~ gauging station~~)~~ in the period 1861 - 2299 under scenarios with and without anthropogenic climate change. The river discharge ~~was~~ is simulated by four hydrological models, HBV, SWAT, SWIM, and VIC driven by four downscaled and bias-corrected GCMs (GFDL-ESM2M, HadGEM2-ES, IPSL-CM5A-LR and MIROC5), and the datasets are available at https://doi.org/10.4121/uuid:8658b22a-8f98-4043-9f8f-d77684d58cbc (Gao et al., 2019).

(1) Scenario without anthropogenic climate change (piControl):

A total of 16 sequences of daily discharge at the Cuntan hydrological station in the upper Yangtze River are ~~the~~ outputs of the four hydrological models that ~~were~~ are driven by the four GCMs in the period 1861 - 2299.

(2) Scenarios with anthropogenic climate change:

Historical period: A total of 16 sequences of daily discharge at the Cuntan station in the upper Yangtze River are ~~the~~ outputs of the four hydrological models that ~~were~~ are driven by the four GCMs in the period 1861 - 2005.

RCP2.6 scenario: a total of 16 sequences of daily runoff at the Cuntan station in the upper Yangtze River are the outputs of the four hydrological models that were driven by the four GCMs in the period 2006 - 2299 (for GFDL-ESM2M, the sequences are for the period 2006 - 2099).

RCP4.5 scenario: a total of 16 sequences of daily discharge at the Cuntan station in the upper Yangtze River are ~~the~~ outputs of the four hydrological models that ~~were~~ are driven by the four GCMs in the period 2006 - 2099 (for IPSL-CM5A-LR, the sequences are for the period 2006 - 2299).

RCP6.0 scenario: a total of 16 sequences of daily discharge at the Cuntan station in the upper Yangtze River are ~~the~~ outputs of the four hydrological models that ~~were~~ are driven by the four GCMs in the period 2006 - 2099.

RCP8.5 scenario: a total of 16 sequences of daily discharge at the Cuntan station in the upper Yangtze River are ~~the~~ outputs of the four hydrological models that ~~were~~ are driven by the four GCMs in the period 2006 - 2099 (for IPSL-CM5A-LR, the sequences are for the period 2006 - 2299).

5 ~~Conclusions and Discussion~~ Summary and conclusions

Using four GCMs (GFDL-ESM2M, HadGEM2-ES, IPSL-CM5A-LR and MIROC5), changes in temperature and precipitation in the upper Yangtze River basin ~~were~~ are analysed from 1861 to the end of 23th century under conditions with anthropogenic climate change ~~(the four RCP scenarios)~~ and for a scenario without ~~human induced~~ anthropogenic climate change (abbreviated as the piControl scenario)~~, and the scenarios were compared~~. The discharge at the Cuntan station in the period 1861 - 2299 ~~was~~ is simulated by four hydrological models (HBV, SWAT, SWIM and VIC) ~~that were~~ driven by the four GCMs, and changes in discharge in a warming world ~~were~~ are compared with those in the piControl scenario.

To ensure the reliability of ~~the~~ simulated runoff ~~data~~, a multi-objective automatic calibration programme using a univariate search technique ~~was~~ is applied to obtain the optimal parameter sets for each hydrological model. For the objective functions, the daily discharge and indicators of high and low flow~~s~~ ~~were~~ are considered. ~~For the calibration,~~ Four criteria, including the NSE, KGE, RSR and r, ~~were~~ are used to evaluate the ~~simulation abilities of the hydrological models~~ parameterization results. To ~~ensure~~ assess the models' ability to satisfactorily ~~represent~~ simulate discharge under different climate conditions, ~~the~~ hydrological models ~~were~~ are ~~additionally~~ validated both in dry and wet periods. ~~In addition~~ Besides, ~~a cross validation method was applied by comparing the evapotranspiration outputs simulated by the hydrological models with the remote sensing based evapotranspiration dataset from the GLEAM.~~ evapotranspiration outputs by simulation process are compared with remote-sensing-based evapotranspiration from the GLEAM dataset to further validate performance of the models.

~~The results showed that the four hydrological models had good performance in the calibration period and in the both dry and wet periods.~~ Previous studies have ~~also~~ shown that ~~the~~ HBV, SWAT and VIC hydrological models could be applied to the Cuntan station in the upper Yangtze River after calibration (Huang et al., 2016； Su et al., 2017; Chen et al., 2017). Our study proves that HBV, SWAT, SWIM and VIC models can satisfactorily simulate precipitation-runoff relation in a changing climate. Moreover, ~~the~~ simulated extreme peak values in the 1930s, 1950s and 1990s ~~were~~ are also in good agreement with the historical documented records of the catastrophic floods in the Yangtze River.

Although the simulation results ~~were~~ are tested ~~and validated with~~ by several criteria, there are still uncertainties that could influence the outputs. These uncertainties are associated with the ~~input~~ GIS data

(e.g., land use data), ~~downscaling~~ selection of the GCMs, ~~and setting the climatic scenarios,~~ the model calibration procedure, and exclusion of water management practices, etc (Gerhard, et al., 2018). First, as no dynamic land use data ~~were~~ are available for the historical period before the 1980s and for the future, a static land use for 1990 ~~was~~ is used for simulating river discharge before ~~(including the piControl period)~~ and after the industrial revolution (historical and RCP scenarios). Second, ~~though~~ although the most up-to-date climate scenarios ~~were~~ are used in this study, downscaling of the GCMs and setting the climate scenarios still contributed to the uncertainty in the hydrological simulation results. Third, the hydrological models were parameterized using the automatic calibration programme. The parameter effects and model applicability ~~were~~ are assessed according to the NSE, KGE, and RSR criteria. However, due to equifinality, there could be other parameter sets that ~~would~~ may result in a similarly good ~~model~~ performance. ~~Actually, the~~ Combination of parameters and not the choice of individual parameters ultimately influences the result (Cheng et al., 2014). There is a lack of analyses on the effects of different parameter combinations in this study, and the uncertainty related to specific parameters in the models needs to be analysed further. Fourth, since the 1990s, human interferences have escalated in the upper Yangtze River. The construction of dikes and reservoirs ~~may~~ alter the timing and volume of peak discharge and ~~low~~ base flow. Without consideration of ~~The~~ effects of human interferences, but rather focus merely on the natural streamflow is one of the limitations in this study ~~were not considered in the modelling, which also might bias the simulation results~~.

The datasets ~~produced~~ generated in our study are the only available long-term and relatively high-precision discharge sequences for the upper Yangtze River, which includes 16 combinations of ~~outputs of~~ four hydrological models that ~~were~~ driven by four GCMs ~~simulations~~. ~~The Simulations of river discharge under the RCP scenarios with anthropogenic climate change and under the piControl scenario without human-induced climate change could provide support for research on climate change and climate change impacts in the upper Yangtze River basin in the period 1861-2299. Additionally, the simulations also provide clues regarding the extent to which human-induced climate change may impact streamflow in the upper Yangtze River.~~ Simulations by multiple hydrological models and GCMs can provide a range of streamflow variations in future, which is a clue for water resource management strategies. According to our simulation results, the daily simulated discharge will be reduced with the decreasing precipitation in the future. Comparison of long-term simulated daily discharge under RCPs with anthropogenic climate change and under the piControl scenario without human-induced climate change can provide support to

understand to which extent human-induced climate change may impact hydrological regime in the upper Yangtze River basin.

Author contribution

Chao Gao, Buda Su, Qianyu Zha, Cai Chen and Gang Luo run the hydrological models. Chao Gao, Buda Su and Tong Jiang analysed results and draft the manuscript. Xiaofan Zeng, Jinlong Huang, Min Xiong and Liping Zhang assisted the data processing. Valentina Krysanova provided guidance for the calibration/validation of the models and the description of results. All authors reviewed the resulting inventory and assisted with paper writing.

Competing interests

The authors declare that they have no conflict of interest.

Acknowledgements

This study was jointly supported by the National Key Research and Development Program of China MOST (2018FY10050001), the National Natural Science Foundation of China (41871024), the High-level Talent Recruitment Program of Ningbo University and the cooperation project between the Natural Science Foundation of China and the Pakistan Science Foundation (41661144027). The authors would like to thank the ISI-MIP project for providing the climate data that was used in this study.

References

Arnold, J. G., Srinivasan, R., Muttiah, R. S., and Williams, J. R.: Large area hydrologic modeling and assessment part I: model development, J Am Water Resour As, 34, 73-89, doi:10.1111/j.1752-1688.1998.tb05961.x, 1998.

Bergström, S. and Forsman, A.: Development of a conceptual deterministic rainfall-runoff model, Hydrol. Res., 4, 147-170, https://doi.org/10.2166/nh.1973.0012, 1973.

Braud, I., Roux, H., Anquetin, S., Maubourguet, M. M., Manus, C., Viallet, P., and Dartus, D.: The use of distributed hydrological models for the Gard 2002 flash flood event: analysis of associated hydrological processes, J. Hydrol., 394, 162-181, https://doi.org/10.1016/j.jhydrol.2010.03.033, 2010.

Changjiang Water Resources Commission of the Ministry of Water Resources: The flood and drought disasters in the Yangtze River Basin, China Water & Power Press, Beijing, China, 2002.

Chen, J., Gao, C., Zeng, X. F., Xiong, M., Wang, Y. J., Jing, C., Krysanova, V., Huang, J. L., Zhao, N., and Su, B. D.: Assessing changes of river discharge under global warming of 1.5°C and 2°C in the upper reaches of the Yangtze River Basin: Approach by using multiple- GCMs and hydrological models, Quat. Int., 453, 63-73, https://doi.org/10.1016/j.quaint.2017.01.017, 2017.

Cheng, X. G., Zhang, J., and Gong, H. L.: HSPF hydrologic simulation and parameter uncertainty in a semi-arid and semi-humid area, Acta Scientiae Circumstantiae, 34, 3179-3187, 2014.

Dahl, T. A., Kendall A. D., and Hyndman, D. W.: Impacts of Projected Climate Change on Sediment Yield and Dredging Costs, Hydrol. Process., 32, 1223-1234, https://doi.org/10.1002/hyp.11486, 2018.

Dufresne, J. L., Foujols, M. A., Denvil, S., Caubel, A., Marti, O., Aumont, O., Balkanski, Y., Bekki, S., Bellenger, H., Benshila, R., Bony, S., Bopp, L., Braconnot, P., Brockmann, P., Cadule, P., Cheruy, F., Codron, F., Cozic, A., Cugnet, D., de Noblet, N., Duvel, J. P., Ethe, C., Fairhead, L., Fichefet, T., Flavoni, S., Friedlingstein, P., Grandpeix, J. Y., Guez, L., Guilyardi, E., Hauglustaine, D., Hourdin, F., Idelkadi, A., Ghattas, J., Joussaume, S., Kageyama, M., Krinner, G., Labetoulle, S., Lahellec, A., Lefebvre, M. P., Lefevre, F., Levy, C., Li, Z. X., Lloyd, J., Lott, F., Madec, G., Mancip, M., Marchand, M., Masson, S., Meurdesoif, Y., Mignot, J., Musat, I., Parouty, S., Polcher, J., Rio, C., Schulz, M., Swingedouw, D., Szopa, S., Talandier, C., Terray, P., Viovy, N., and Vuichard, N.: Climate change projections using the IPSL-CM5 Earth System Model: from CMIP3 to CMIP5, Clim. Dyn., 40, 2123-2165, https://doi.org/10.1007/s00382-012-1636-1, 2013.

Frieler, K., Lange, S., Piontek, F., Reyer, C. P. O., Schewe, J., Warszawski, L., Zhao, F., Chini, L., Denvil, S., Emanuel, K., Geiger, T., Halladay, K., Hurtt, G., Mengel, M., Murakami, D., Ostberg, S., Popp, A., Riva, R., Stevanovic, M., Suzuki, T., Volkholz, J., Burke, E., Ciais, P., Ebi, K., Eddy, T. D., Elliott, J., Galbraith, E., Gosling, S. N., Hattermann, F., Hickler, T., Hinkel, J., Hof, C., Huber, V., Jägermeyr, J., Krysanova, V., Marcé, R., Schmied, H. M., Mouratiadou, I., Pierson, D., Tittensor, D. P., Vautard, R., Vliet, M., Biber, M. F., Betts, R. A., Bodirsky, B. L., Deryng, D., Frolking, S., Jones, C. D., Lotze, H. K., Lotze-Campen, H., Sahajpal, R., Thonicke, K., Tian, H. Q., and Yamagata, Y.: Assessing the impacts of 1.5 °C global warming – simulation protocol of the Inter-Sectoral Impact Model Intercomparison Project (ISIMIP2b), Geosci. Model Dev., 10, 4321-4345, https://doi.org/10.5194/gmd-10-4321-2017, 2017.

Gao, C., Su, B.D., Krysanova V., Zha Q.Y., Chen C., Luo G., Zeng X.F., Huang J.L., Xiong M., Zhang

L.P, Jiang T.: A 439-year daily discharge dataset (1861-2299) for the upper Yangtze River, China. 4TU.ResearchData, https://doi.org/10.4121/uuid:8658b22a-8f98-4043-9f8f-d77684d58cbc, 2019.

Gerhard, K. and Flanner, M. G.: Striking stationarity of large-scale climate model bias patterns under strong climate change, Proc. Natl. Acad. Sci. U. S. A., 115, 9462-9466, https://doi.org/10.1073/pnas.1807912115, 2018.

Gupta, H. V., Kling, H., Yilmaz, K. K., and Martinez, G. F.: Decomposition of the mean squared error and NSE performance criteria: implications for improving hydrological modelling, J. Hydrol., 377, 80-91, https://doi.org/10.1016/j.jhydrol.2009.08.003, 2009.

Hattermann, F. F., Krysanova, V., Gosling, S. N., Dankers, R., Daggupati, P., Donnelly, C., Floerke, M., Huang, S., Motovilov, Y., Buda, S., Yang, T., Mueller, C., Leng, G., Tang, Q., Portmann, F. T., Hagemann, S., Gerten, D., Wada, Y., Masaki, Y., Alemayehu, T., Satoh, Y., and Samaniego, L.: Cross-scale intercomparison of climate change impacts simulated by regional and global hydrological models in eleven large river basins, Clim. Change, 141, 561-576, https://doi.org/10.1007/s10584-016-1829-4, 2017.

Hu, M.S. and Luo, C.Z: The historical flood of China, China Bookstore press, Beijing, China, 1992.

Huang, J. L., Wang, Y. J., Su, B., and Zhai, J. Q.: Future Climate Change and Its Impact on Runoff in the Upper Reaches of the Yangze River Under RCP4.5 Scenario, Meteorological Monthly, 42, 614-620, https://doi.org/10.7519/j.issn.1000-0526.2016.05.011, 2016.

Jones, C. D., Hughes, J. K., Bellouin, N., Hardiman, S. C., Jones, G. S., Knight, J., Liddicoat, S., O'Connor, F. M., Andres, R. J., Bell, C., Boo, K. O., Bozzo, A., Butchart, N., Cadule, P., Corbin, K. D., Doutriaux-Boucher, M., Friedlingstein, P., Gornall, J., Gray, L., Halloran, P. R., Hurtt, G., Ingram, W. J., Lamarque, J. F., Law, R. M., Meinshausen, M., Osprey, S., Palin, E. J., Chini, L. P., Raddatz, T., Sanderson, M. G., Sellar, A. A., Schurer, A., Valdes, P., Wood, N., Woodward, S., Yoshioka, M., and Zerroukat, M.: The HadGEM2-ES implementation of CMIP5 centennial simulations, Geosci. Model Dev., 4, 543-570, https://doi.org/10.5194/gmd-4-543-2011, 2011.

Jung, I. W., Chang, H., and Moradkhani, H.: Quantifying uncertainty in urban flooding analysis considering hydro-climatic projection and urban development effects, Hydrol. Earth Syst. Sci, 15, 617-633, http://doi.org/10.5194/hess-15-617-2011, 2011.

Krysanova V., Donnelly Ch., Gelfan A., Gerten D., Arheimer B., Hattermann F., and Kundzewicz Z.: How the performance of hydrological models relates to credibility of projections under climate

change, Hydrolog SCI J., 63, 696-720, https://doi.org/10.1080/02626667.2018.1446214, 2018.

Krysanova V., Hattermann F., and Wechsung F.: Development of the ecohydrological model SWIM for regional impact studies and vulnerability assessment, Hydrol. Process, 19, 763–783, https://doi.org/10.1002/hyp.5619, 2005.

Lai, C., Reinders, M. J. T., and Wessels, L.: Random subspace method for multivariate feature selection, Pattern. Recogn. Lett., 27, 1067-1076, https://doi.org/10.1016/j.patrec.2005.12.018, 2006.

Lange, S.: Bias correction of surface downwelling longwave and shortwave radiation for the EWEMBI dataset, Earth. Syst. Dynam., 9, 627-645, https://doi.org/10.5194/esd-2017-81, 2018.

Liang, X., Lettenmaier, D. P., Wood, E. F., and Burges, S. J.: A simple hydrologically based model of land surface water and energy fluxes for general circulation models, J. Geophys. Res.-Atmos., 99, 14415–14428, https://doi.org/10.1029/94JD00483, 1994.

Longfield, S. A., Faulkner, D., Kjeldsen, T. R., Macklin, M. G., Jones, A. F., Foulds, S. A., Brewer, P. A., Griffiths, H. M.: Incorporating sedimentological data in UK flood frequency estimation, J. Flood Risk Manag., e12449, https://doi.org/10.1111/jfr3.12449, 2018.

Luo, C.Z. and Le, J.X: The flood of China, China Bookstore press, Beijing, China, 1996.

Maisa, R., Fabrice, L., Julian, R. V., and Andrew, J. C.: Emergence of robust precipitation changes across crop production areas in the 21st century, Proc. Natl. Acad. Sci. U. S. A., 116, 6673-6678, https://doi.org/10.1073/pnas.1811463116, 2019.

Meaurio, M., Zabaleta, A., Boithias, L., Epelde, A. M., Sauvage, S., Sanchez-Perez, J. M., Srinivasan, R., and Autiguedad, I: Assessing the hydrological response from an ensemble of CMIP5 climate projections in the transition zone of the Atlantic region (Bay of Biscay), J. Hydrol., 548, 46-62, https://doi.org/10.1016/j.jhydrol.2017.02.029, 2017.

Miralles, D. G., Holmes, T. R. H., De, J. R. A. M., Gash, J. H., Meesters, A. G. C. A., and Dolman, A. J.: Global land-surface evaporation estimated from satellite-based observations, Hydrol. Earth Syst. Sci., 15, 453-469, https://doi.org/10.5194/hess-15-453-2011, 2011

Moriasi, D. N., Arnold, J. G., Van Liew, M. W., Bingner, R. L., Harmel, R. D., and Veith, T. L.: Model evaluation guidelines for systematic quantification of accuracy in watershed simulations, T. Asabe, 50, 885-900, https://doi.org/10.13031/2013.23153, 2007.

Nash, J. E., and Sutcliffe, J. V.: River flow forecasting through conceptual models part I — A discussion of principles, J. Hydrol., 10, 282-290, https://doi.org/10.1016/0022-1694(70)90255-6, 1970.

Raman Vinna, L., Wuest, A., Zappa, M., Fink, G., and Bouffard, D.: Tributaries affect the thermal response of lakes to climate change, Hydrol. Earth Syst. Sci., 22, 1-40, https://doi.org/10.5194/hess-22-31-2018, 2018.

Ren, Z. H., Zhao, P., Zhang, Q., Zhang, Z. F., Cao, L. J., Yang, Y. R., Zou, F. L., Zhao, Y. F., Zhao, H. M., Chen, Z.: Quality control procedures for hourly precipitation data from automatic weather stations in China, Meteorological Monthly, 36, 123–132, https://doi.org/10.3788/HPLPB20102207.1462,2010. (in Chinese)

Seneviratne, S. I., Rogelj, J., Seferian, R., Wartenburger, R., Allen, M. R., Cain, M., Millar, R. J., Ebi, K. L., Ellis, N., Hoegh-Guldberg, O., Payne, A. J., Schleussner, C. F., Tschakert, P., Warren, R. F.: The many possible climates from the Paris Agreement's aim of 1.5 degrees C warming, Nature, 558, 41-49, https://doi.org/10.1038/s41586-018-0181-4, 2018.

Stagl, J. C. and Hattermann, F. F.: Impacts of climate change on riverine ecosystems: Alterations of ecologically relevant flow dynamics in the danube river and its major tributaries, Water, 8, 566, https://doi.org/10.3390/w8120566, 2016.

Su, B., Gemmer, M., and Jiang, T.: Spatial and temporal variation of extreme precipitation over the Yangtze River Basin, Quat. Int., 186, 22-31, https://doi.org/10.1016/J.QUAINT.2007.09.001, 2008.

Su, B., Huang, J. L., Zeng, X. L., Gao, C., and Jiang, T.: Impacts of climate change on streamflow in the upper Yangtze River basin, Clim. Change, 141, 533-546, https://doi.org/10.1007/s10584-016-1852-5, 2017.

Su, B., Zeng X. F., Zhai, J. Q., Wang, Y. J., and Li, X. C.: Projected precipitation and streamflow under SRES and RCP emission scenarios in the Songhuajiang River basin, China, Quat. Int., 380, 95-105, https://doi.org/10.1016/j.quaint.2014.03.049, 2015.

Taylor, K. E., Stouffer R. J., and Meehl G. A.: An Overview of CMIP5 and the Experiment Design, B. Am. Meteorol. Soc., 93, 485-498, https://doi.org/10.1175/BAMS-D-11-00094.1, 2012.

Thomas, F., Marco, G., Liu, L., Su, B.: Change-points in climate extremes in the Zhujiang River Basin, South China, 1961–2007, J. Clim., 110: 783-799, https://doi.org/10.1007/s10584-011-0123-8, 2012.

Wang, G. J., Jiang, T., Blender, R., and Fraedrich, K.: Yangtze 1/f discharge variability and the interacting river–lake system, J. Hydrol., 351, 230-237, https://doi.org/10.1016/j.jhydrol.2007.12.016, 2008.

Watanabe, M., Suzuki, T., O'ishi, R., Komuro, Y., Watanabe, S., Emori, S., Takemura, T., Chikira, M., Ogura, T., Sekiguchi, M., Takata, K., Yamazaki, D., Yokohata, T., Nozawa, T., Hasumi, H., Tatebe,

H., and Kimoto, M.: Improved climate simulation by MIROC5: mean states, variability, and climate sensitivity, J. Clim., 23, 6312-6335, https://doi.org/10.1175/2010JCLI3679.1, 2010.

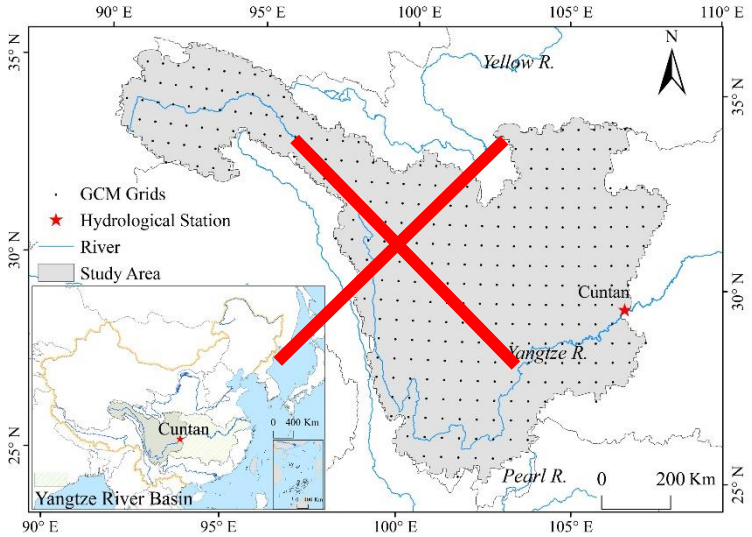

~~**Figure 1: Location of the Cuntan hydrological station and the GCM grids in the upper Yangtze River basin**~~

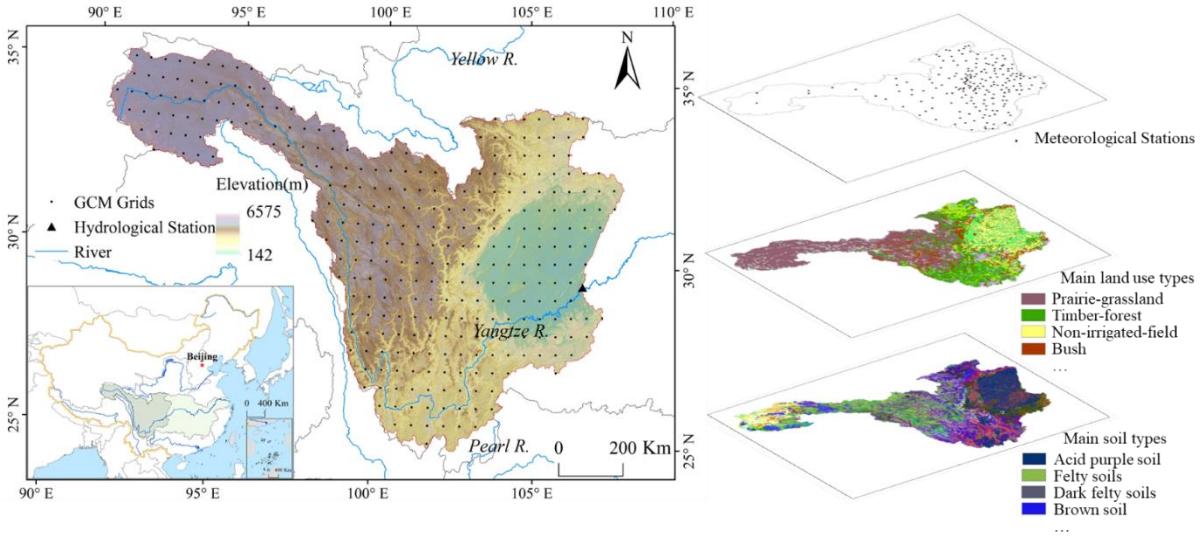

Figure 1 Location of the Cuntan hydrological station, GCM grids, meteorological stations and spatial distribution of the land use and soil types in the upper Yangtze River basin

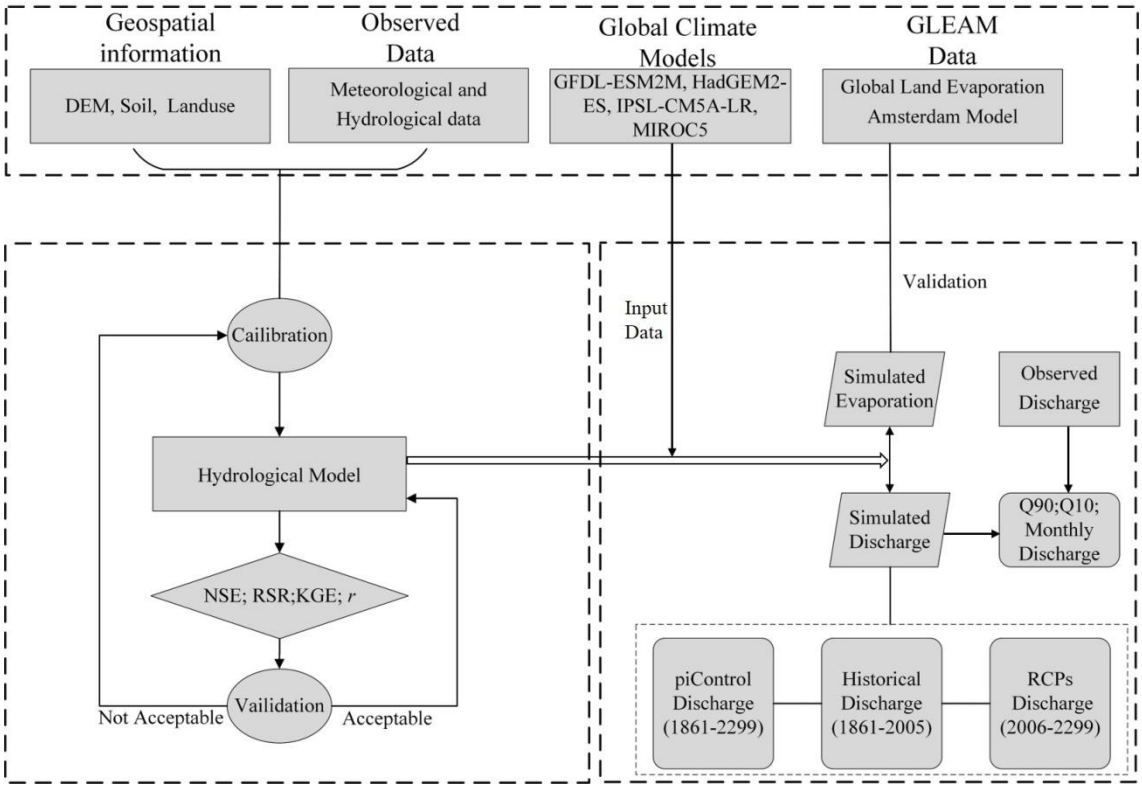

Figure 2 Flowchart for hydrological modelling process

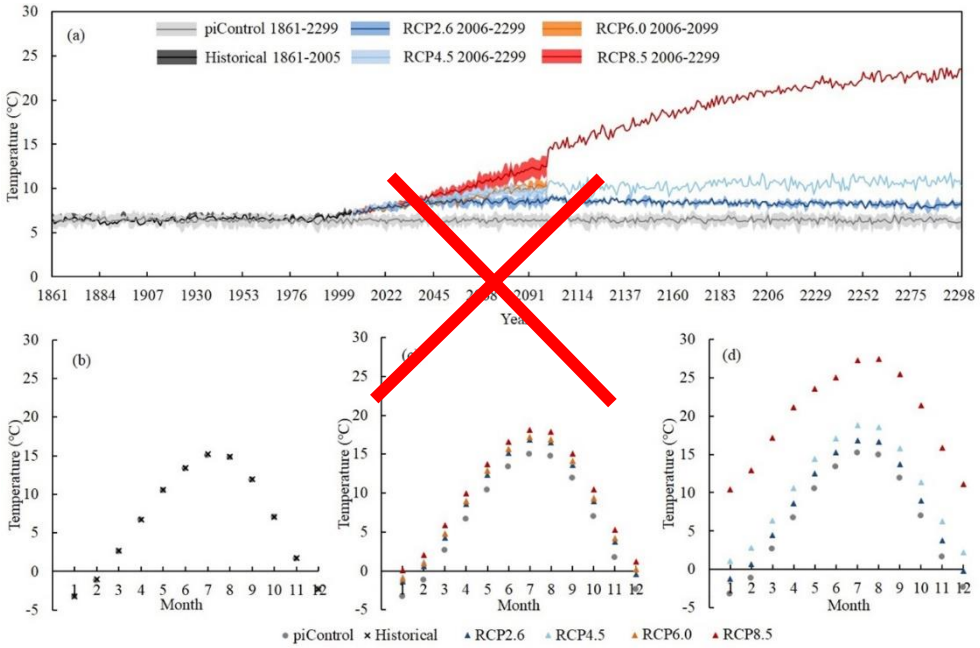

~~**Figure 2: Interannual (a) and long-term average seasonal (b-d) dynamics of the surface air temperature in the upper Yangtze basin: comparison of the piControl scenario with the historical and anthropogenic climate change RCP scenarios (periods: a: 1861-2299; b: 1861-2005; c: 2006-2099; and d: 2100-2299)**~~

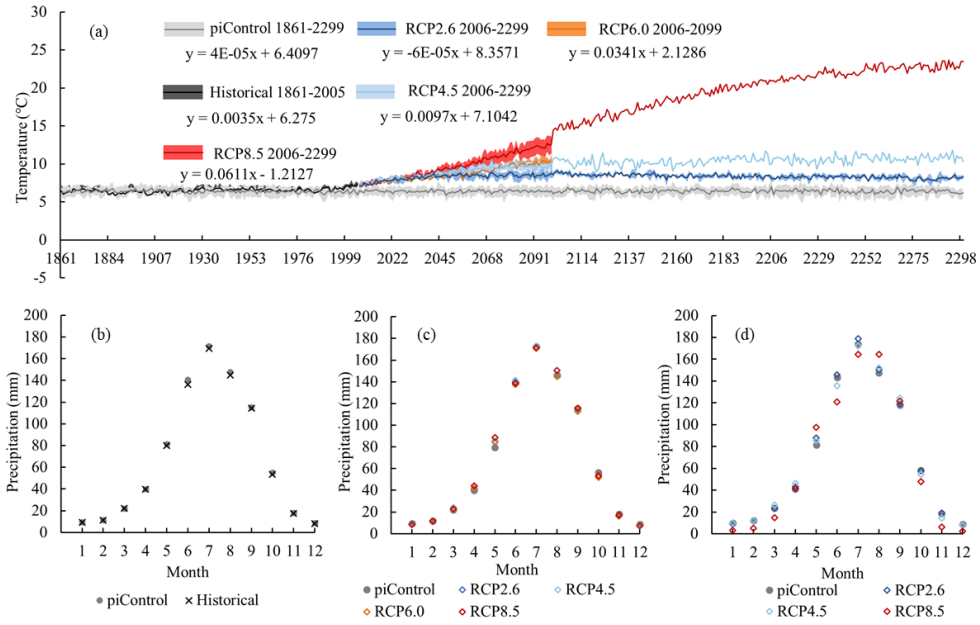

Figure 3 Inter-annual (a) and long-term averaged monthly dynamics (b-d) of the surface air temperature in the upper Yangtze River basin: comparison of the piControl scenario with the anthropogenic climate change scenarios (periods: a: 1861 - 2299; b: 1861 - 2005; c: 2006 - 2099; and d: 2100 - 2299)

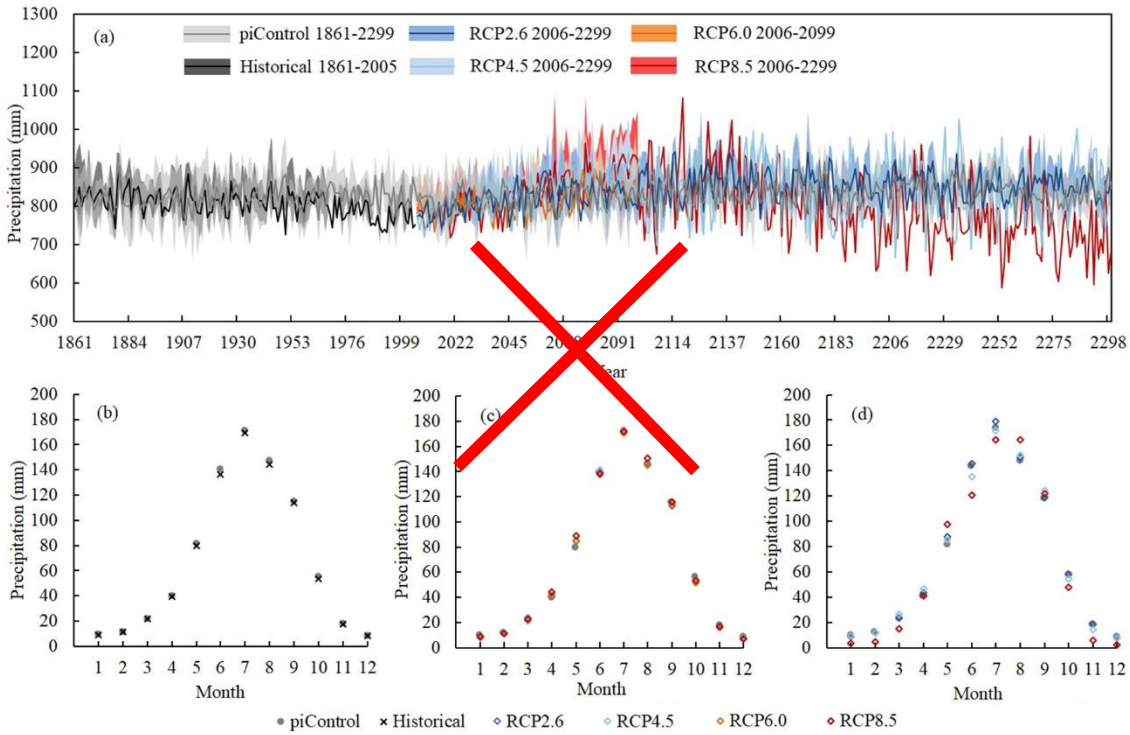

Figure 3: Annual (a) and long-term average seasonal (b-d) dynamics of precipitation in the upper Yangtze basin: comparison of the piControl scenario with the historical and anthropogenic climate change RCP scenarios (periods: a: 1861-2299; b: 1861-2005; c: 2006-2099; and d: 2100-2299)

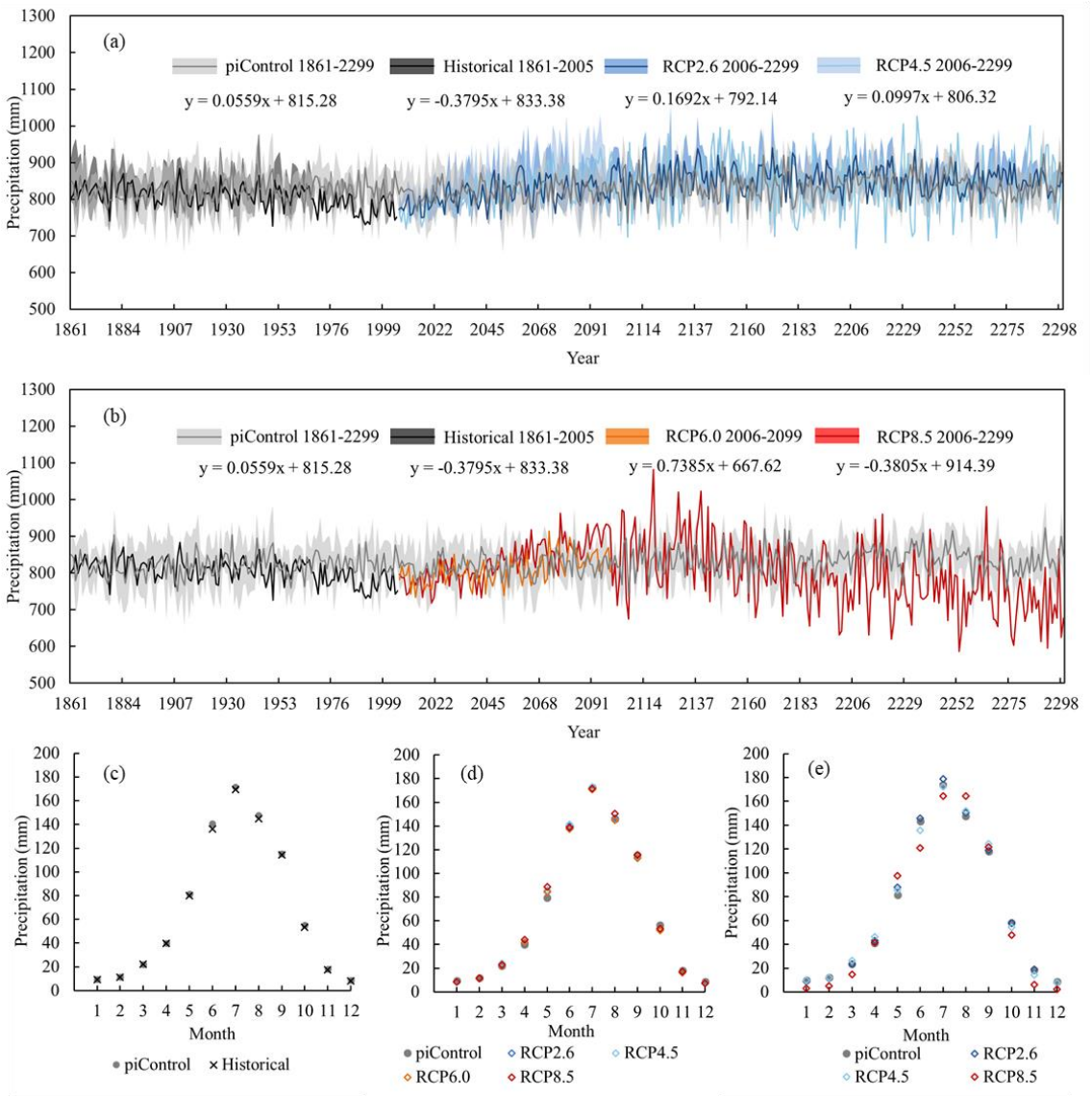

Figure 4 Inter-annual (a-b) and long-term averaged monthly dynamics (c-e) of precipitation in the upper Yangtze River basin: comparison of the piControl scenario with the anthropogenic climate change scenarios (periods: a: 1861-2299; b: 1861-2299; c: 1861 - 2005; d: 2006 - 2099; and e: 2100 - 2299)

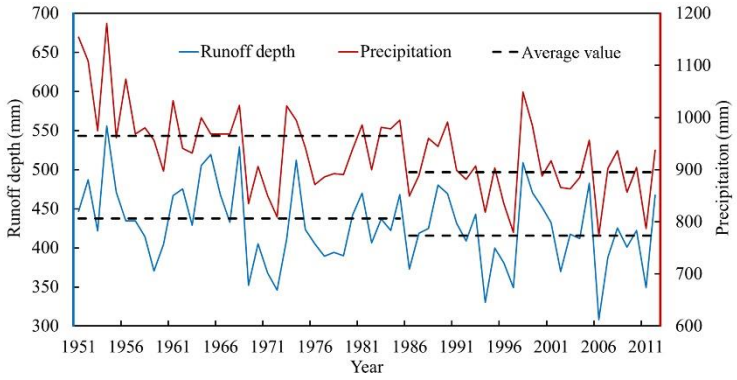

~~Figure 4~~ Figure 5 **Annual precipitation and runoff depth observed in the upper Yangtze River basin in the period 1951 - 2012**

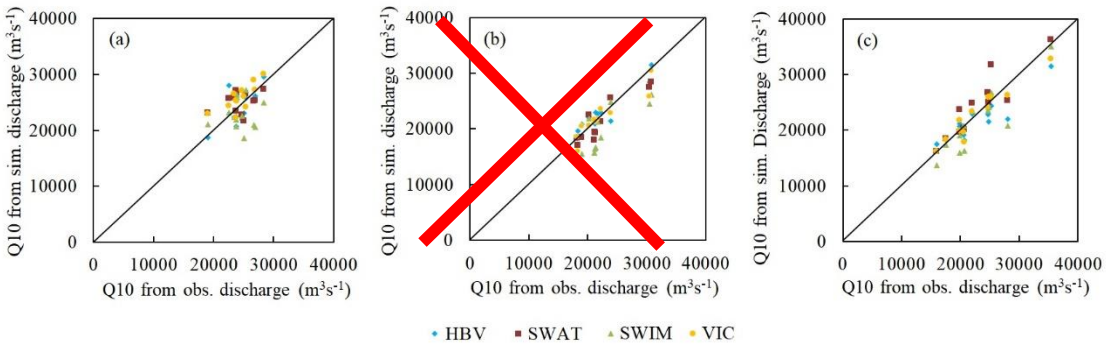

~~**Figure 5: Comparison of the Q10 values based on the simulated and observed discharge data at the Cuntan station in the calibration period, 1979-1990, (a) and validation periods, 1967-1978 (b) and 1991-2002 (c)**~~

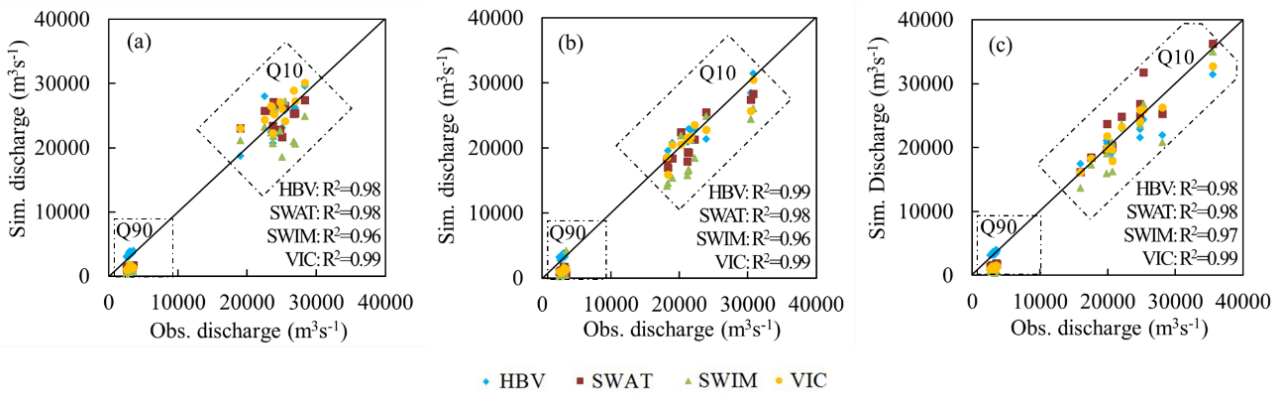

Figure 6 Comparison of the simulated and observed Q10, Q90 percentiles at the Cuntan station in the calibration period 1979 - 1990 (a) and validation period 1967 - 1978 and 1991 - 2002 (b-c)

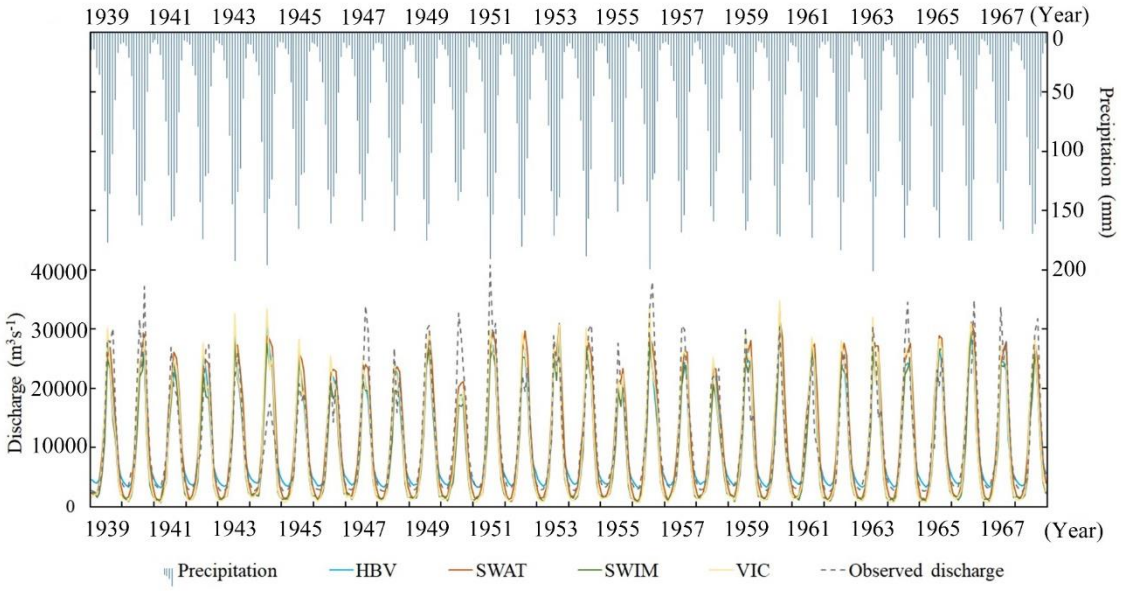

~~Figure 6~~ Figure 7 Observed and simulated monthly discharge and precipitation at the Cuntan station in the upper Yangtze basin in the period 1939 - 1968

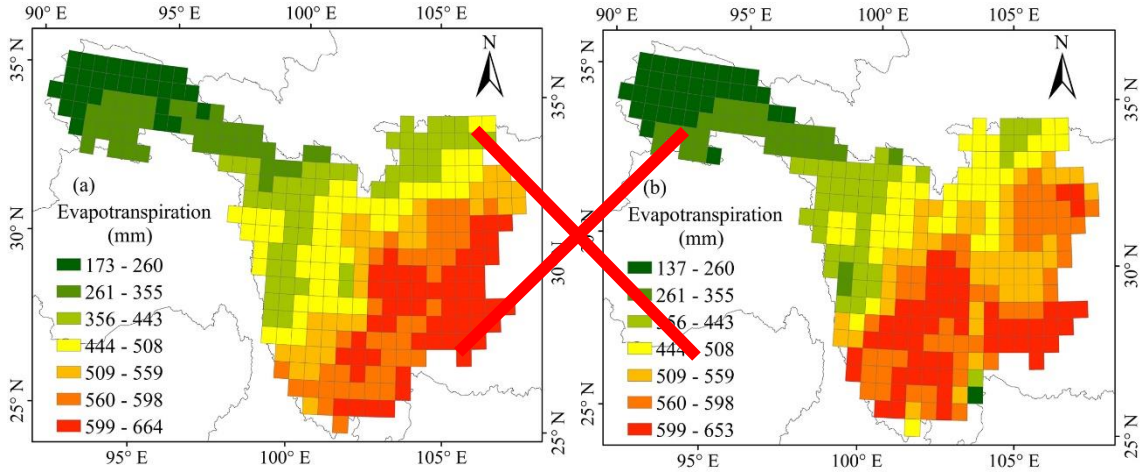

~~**Figure 7: Spatial distribution of the mean annual evapotranspiration in the upper Yangtze River basin in the period 1986-2005 based on outputs from the hydrological model VIC (a) and GLEAM (b)**~~

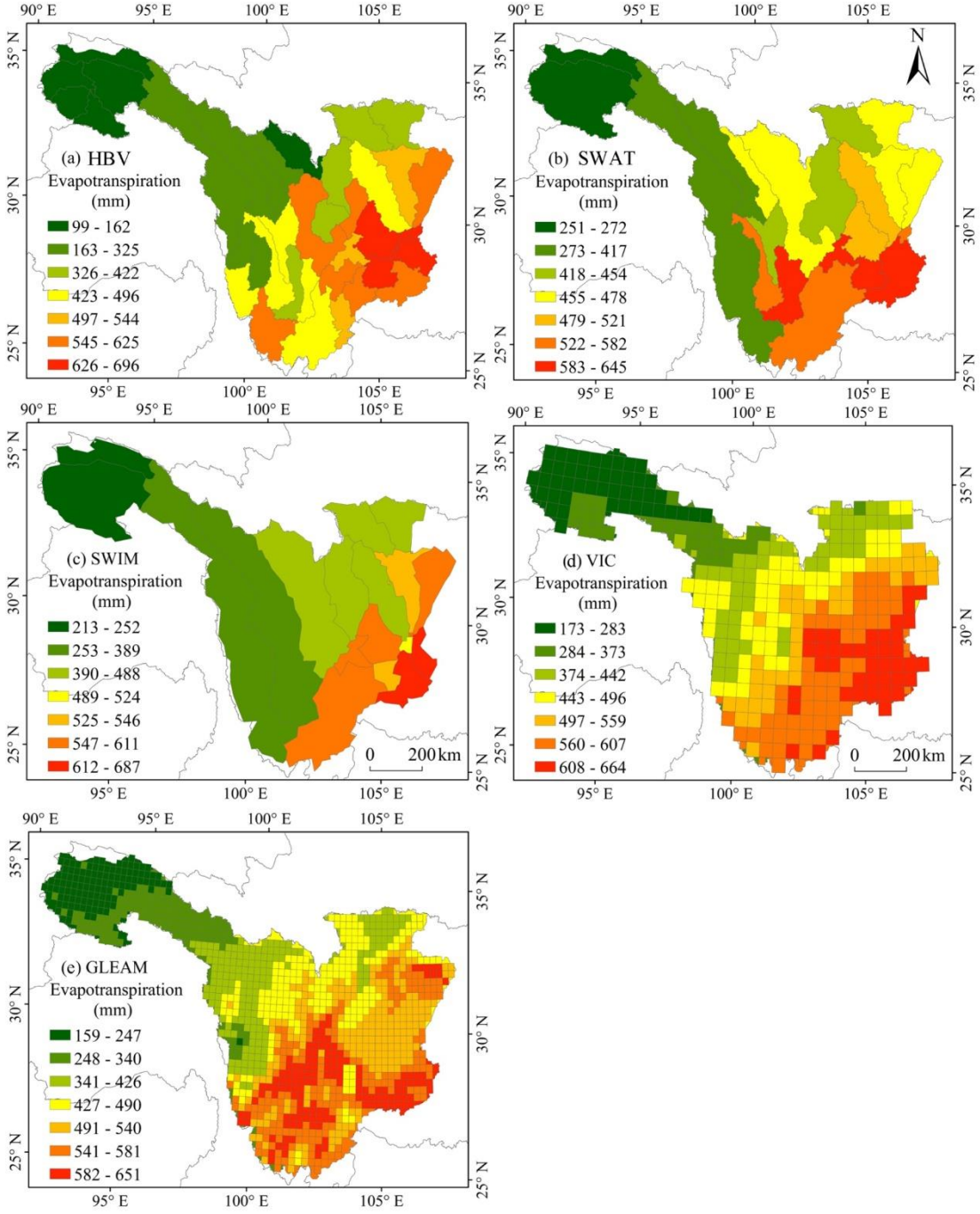

Figure 8 Spatial distribution of multi-year averaged annual evapotranspiration in the upper Yangtze River basin for 1986 - 2005: HBV output (a), SWAT output (b), VIC output (c), SWIM output (d) and GLEAM data(e)

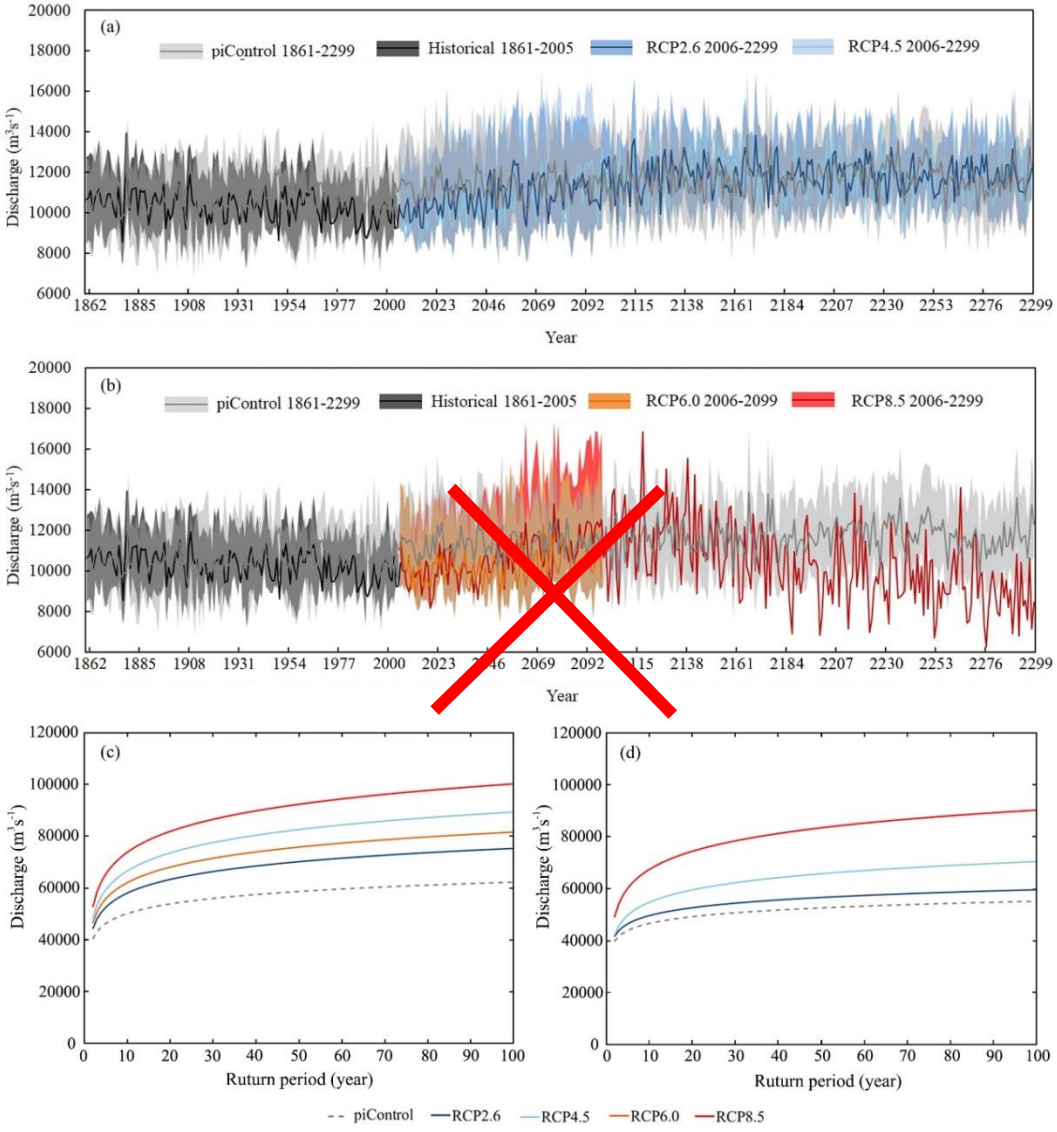

Figure 8: The annual mean discharge under the piControl scenario and scenarios with anthropogenic climate change effects simulated by the four hydrological models (SWIM, SWAT, HBV, and VIC) (a-b) and the return periods of daily maximum discharge (c-d) at the Cuntan station; comparison of the piControl scenario with the anthropogenic climate change RCP scenarios (periods: a-b: 1861-2299; c: 2070-2099; and d: 2170-2199)

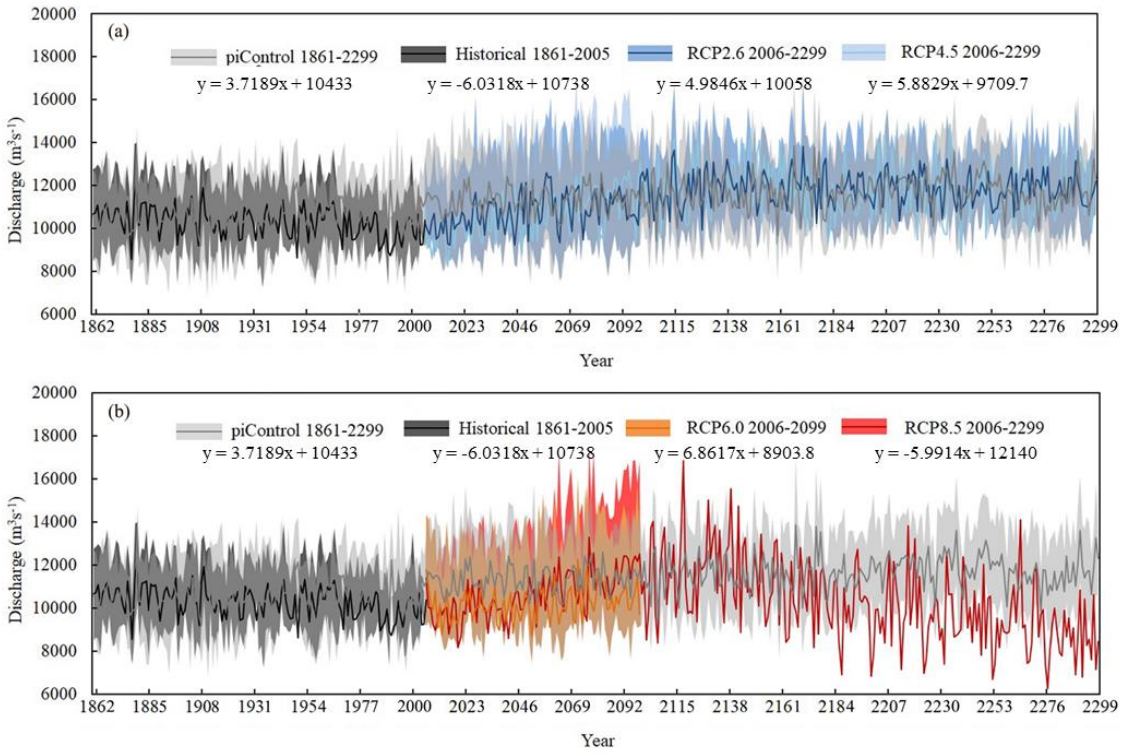

Figure 9 The annual mean discharge at the Cuntan station simulated by four hydrological models (HBV, SWAT, SWIM, and VIC) under the piControl scenario and scenarios with anthropogenic climate change effects (a-b)

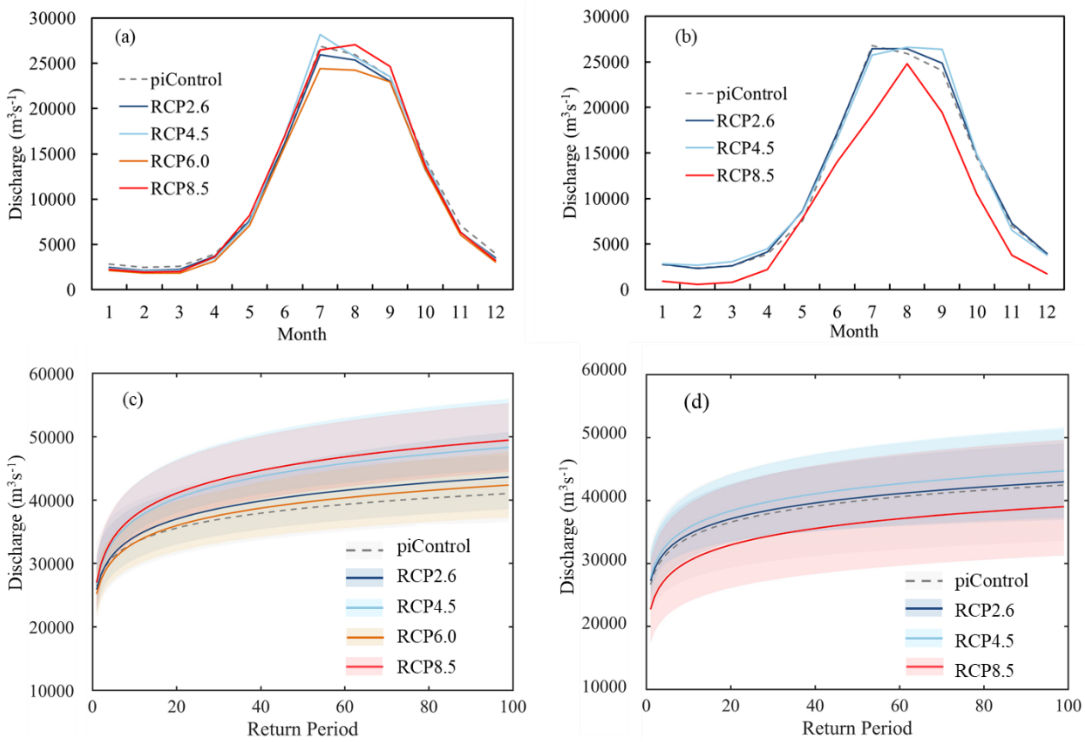

Figure 10 Comparison of monthly mean simulated discharge and return periods of daily maximum discharge at the Cuntan station for 2070 - 2099 (a, c) and 2270 - 2299 (b, d) under RCPs and the piControl scenario

Table 1 Availability of climate scenarios from four GCMs for different periods

Climate scenario	CO_2 concentration	GFDL-ESM2M	HadGEM2-ES	IPSL-CM5A-LR	MIROC5
piControl scenario	286 ppm	1861-2099	1861-2299	1861-2299	1861-2299
Historical scenario	Recorded CO_2	1861-2005	1861-2005	1861-2005	1861-2005
Future scenario	RCP2.6	2006-2099	2006-2299	2006-2299	2006-2299
	RCP4.5	2006-2099	2006-2099	2006-2299	2006-2099
	RCP6.0	2006-2099	2006-2099	2006-2099	2006-2099
	RCP8.5	2006-2099	2006-2099	2006-2299	2006-2099

Table 2 Short description of HBV, SWAT, SWIM, and VIC

Model	Developed Institution	Spatial disaggregation	Representation of soils	Representation of vegetation	Routing method
HBV	Swedish Meteorological and Hydrological Institution	Sub-basins, 10 elevation zones & land use classes	1 soil layer, 2 soil parameters	Fixed monthly plant characteristics	A simple time-lag method
SWAT	United States Department of Agriculture	Sub-basins and hydrological response units	Up to 10 soil layers, 11 soil parameters	A simplified EPIC approach	Muskingum method
SWIM	The Potsdam Institute for Climate Impact Research, based on the SWAT and MATSALU models	Sub-basins and hydrotopes	Up to 10 soil layers, 11 soil parameters	A simplified EPIC approach	Muskingum method, reservoirs and irrigation
VIC	University of Washington, University of California, and Princeton University	Grid of large and uniform cells with sub-grid heterogeneity	3 soil layers, 19 parameters	Fixed monthly plant characteristics	Linearized St. Venant's equations

Table 3 The parameters and their ranges used for calibration of four hydrological models

HBV Name	Range	SWAT Name	Range	SWIM Name	Range	VIC Name	Range
Threshold quick runoff (UZ1)	0-100	Deep aquifer percolation fraction (*Rchrg_Dp*)	0-1	Routing coefficient 1 (*roc1*)	1-100	Non-linear baseflow begins (*Ds*)	0-1
Percolation to lower zone (*PREC*)	0-6	Saturated hydraulic conductivity (*Sol_K*)	0-100	Routing coefficient 2 (*roc2*)	1-100	Maximum baseflow (Ds_{max})	0-30
Non-linearity in soil water zone (*BETA*)	1-5	Maximum canopy storage (*Canmx*)	0-10	Evaporation coefficient (*thc*)	0.5-1.5	Maximum soil moisture (*Ws*)	0-1
Slow time constant upper zone (*KUZ1*)	0.01-1	Average slope steepness (*Slope*)	0-0.6	Baseflow factor for return flow travel time (*bff*)	0.2-1	Variable Infiltration Capacity curve (b_i)	0-0.4
Additional precipitation coefficient for snow at gauge (*SKORR*)	1-3	Available water capacity (*Sol_Awc*)	0-1	Coefficient to correct channel width (*chwc0*)	0.1-1	Soil depth 1 (d_1)	0.1-1
Precipitation correction for rain (*PKORR*)	0.8-3	Initial SCS CN II value (*Cn2*)	35-98	Saturated conductivity (*sccor*)	0.01-10	Soil depth 2 (d_2)	0.1-2
		Groundwater "revap" coefficient (*Gw_Revap*)	0.02-0.2	Groundwater recession rate (*abf*)	0.01-1	Soil depth 3 (d_3)	0.1-3
		Biological mixing efficiency (*Biomix*)	0-1	Initial conditions (*gwq0*)	0.01-1		
		Soil evaporation compensation factor (*Esco*)	0-1	Curve number (*cnum*)	10-100		

~~Table 3: Evaluation criteria for testing performance of hydrological models~~

Criterion	Formula	Range	Ideal value	Notation
Nash-Sutcliffe efficiency (NSE)	$1-\frac{\sum_{t=1}^{N}(Q_{s,t}-Q_{o,t})^2}{\sum_{t=1}^{N}(Q_{o,t}-\bar{Q}_o)^2}$	(-∞, 1)	1	Q_s: simulated discharge; Q_o: observed discharge; $\bar{Q}_o$: mean of observed discharge; $\bar{Q}_s$: mean of simulated discharge; t: sequence of the discharge series; N: number of time steps; α: ratio between the standard deviations of the simulated and observed data; β: ratio between the mean simulated and mean observed discharge
Ratio of the root mean square error and the standard deviation of observation (RSR)	$\frac{\sqrt{\sum_{t=1}^{N}(Q_{o,t}-Q_{s,t})^2}}{\sqrt{\sum_{t=1}^{N}(Q_{o,t}-\bar{Q}_o)^2}}$	(0, +∞)	0	
Pearson's correlation coefficient (r)	$\frac{\sum_{t=1}^{N}(Q_{s,t}-\bar{Q}_s)(Q_{o,t}-\bar{Q}_o)}{\sqrt{\sum_{t=1}^{N}(Q_{s,t}-\bar{Q}_s)^2}-\sqrt{\sum_{t=1}^{N}(Q_{o,t}-\bar{Q}_o)^2}}$	(-1, 1)	1	
Modified Kling -Gupta efficiency (KGE)	$1-\sqrt{(\alpha-1)^2+(\beta-1)^2+(r-1)^2}$	(-∞, 1)	1	

Table 4 Evaluation criteria for testing simulation capacity of hydrological models

Criterion	Formula	Range	Ideal value	Notation	Reference
Nash-Sutcliffe efficiency (NSE)	$1-\frac{\sum_{t=1}^{N}(Q_{s,t}-Q_{o,t})^2}{\sum_{t=1}^{N}(Q_{o,t}-\bar{Q}_o)^2}$	(-∞, 1)	1	Q_s: simulated discharge; Q_o: observed discharge; $\bar{Q}_o$: mean of observed discharge; $\bar{Q}_s$: mean of simulated discharge; t: sequence of the discharge series; N: number of time steps; α: ratio between the standard deviations of the simulated and observed data; β: ratio between the mean simulated and mean observed discharge	(Nash and Sutcliffe, 1970)
Ratio of the root mean square error and the standard deviation of observation (RSR)	$\frac{\sqrt{\sum_{t=1}^{N}(Q_{o,t}-Q_{s,t})^2}}{\sqrt{\sum_{t=1}^{N}(Q_{o,t}-\bar{Q}_o)^2}}$	(0, +∞)	0		(Moriasi et al., 2007)
Pearson's correlation coefficient (r)	$\frac{\sum_{t=1}^{N}(Q_{s,t}-\bar{Q}_s)(Q_{o,t}-\bar{Q}_o)}{\sqrt{\sum_{t=1}^{N}(Q_{s,t}-\bar{Q}_s)^2}-\sqrt{\sum_{t=1}^{N}(Q_{o,t}-\bar{Q}_o)^2}}$	(-1, 1)	1		(Huang et al., 2012)
Modified Kling-Gupta efficiency (KGE)	$1-\sqrt{(\alpha-1)^2+(\beta-1)^2+(r-1)^2}$	(-∞, 1)	1		(King et al., 2012)

Table 5 Mean values of temperature, precipitation and simulated discharge in different scenarios

		piControl scenario	Historical scenario	Future scenario			
				RCP2.6	RCP4.5	RCP6.0	RCP8.5
Temperature (℃)	1861-2005	6.40	6.53	-	-	-	-
	2006-2099	6.41	-	8.27	8.79	8.70	9.72
	2100-2299	6.43	-	8.38	10.48	-	19.94
Precipitation (mm)	1861-2005	821.8	805.7	-	-	-	-
	2006-2099	819.2	-	814.9	823.8	809.8	830.2
	2100-2299	835.7	-	854.2	841.0	-	790.4
Discharge (m^3s^{-1})	1861-2005	10578.0	10294.4	-	-	-	-
	2006-2099	11338.6	-	10784.6	10592.6	10224.6	10617.8
	2100-2299	11698.5	-	11859.2	11824.3	-	10279.2

~~Table 4: Criteria of fit of the four hydrological models in the calibration period and in the wet and dry validation periods~~

Table 6 Performance of four hydrological models in the upper Yangtze River at the calibration period and the wet and dry validation periods

Criterion	Threshold	Calibration/validation	HBV	SWAT	SWIM	VIC
		1979-1990	0.86	0.81	0.75	0.89
NSE	>=0.7	1967-1978 (wet period)	0.86	0.79	0.7	0.88
		1991-2002 (dry period)	0.86	0.81	0.75	0.89
		1979 - 1990	0.39	0.43	0.50	0.33
RSR	<=0.6	1967-1978 (wet period)	0.38	0.46	0.55	0.34
		1991-2002 (dry period)	0.36	0.42	0.48	0.32
		1979-1990	0.92	0.91	0.91	0.97
r	>=0.9	1967-1978 (wet period)	0.92	0.90	0.89	0.96
		1991-2002 (dry period)	0.94	0.92	0.93	0.97
		1979-1990	0.87	0.9	0.7	0.71
KGE	>=0.7	1967-1978 (wet period)	0.90	0.88	0.65	0.69
		1991-2002 (dry period)	0.85	0.89	0.56	0.68

~~**Table 5: Comparison of changes in the mean annual discharge, Q10 and Q90 in the period 2006-2299 under the scenarios of anthropogenic climate change and the piControl scenario**~~

~~Dataset~~	~~Rate of change (Mean) (%)~~	~~Rate of change (Q10) (%)~~	~~Rate of change (Q90) (%)~~	~~Standard deviation~~	~~Coefficient of variation~~
~~piControl~~	~~-~~	~~-~~	~~-~~	~~980.4~~	~~0.08~~
~~RCP2.6~~	~~-0.92~~	~~-0.49~~	~~-3.8~~	~~1146.2~~	~~0.10~~
~~RCP4.5~~	~~-4.7~~	~~5.2~~	~~-11.9~~	~~1819.6~~	~~0.17~~
~~RCP6.0~~	~~-7.7~~	~~-7.3~~	~~-7.9~~	~~965.9~~	~~0.09~~
~~RCP8.5~~	~~-18.2~~	~~-2.9~~	~~-30.6~~	~~2347.9~~	~~0.25~~

Table 7 Relative changes in mean annual discharge, Q10 and Q90 in the periods 2070 - 2099 and 2270 - 2299 under the scenarios of anthropogenic climate change relative to the piControl scenario

Period	Scenarios	Relative change of mean discharge (%)	Relative change of Q10 (%)	Relative change of Q90 (%)	Standard deviation	Coefficient of variation
2070-2099	piControl	-	-	-	607.1	0.05
	RCP2.6	-4.2	-1.2	-5.4	681.1	0.06
	RCP4.5	-1.1	3.2	-10.9	997.1	0.09
	RCP6.0	-9.1	-3.5	-10.6	763.7	0.07
	RCP8.5	-0.7	4.3	-3.5	917.3	0.08
2270-2299	piControl	-	-	-	767.6	0.06
	RCP2.6	2.2	2.5	3.2	608.8	0.05
	RCP4.5	2.6	6.6	-2.3	1255.9	0.11
	RCP6.0	-	-	-	-	-
	RCP8.5	-30.6	-13.2	-50.4	1397.4	0.16